

Copyright © 1993, by the author(s).  
All rights reserved.

Permission to make digital or hard copies of all or part of this work for personal or classroom use is granted without fee provided that copies are not made or distributed for profit or commercial advantage and that copies bear this notice and the full citation on the first page. To copy otherwise, to republish, to post on servers or to redistribute to lists, requires prior specific permission.

**TWO-PARAMETER STUDY OF TRANSITION  
TO CHAOS IN CHUA'S CIRCUIT:  
RENORMALIZATION GROUP, UNIVERSALITY  
AND SCALING**

by

A. P. Kuznetsov, S. P. Kuznetsov, I. R. Sataev,  
and L. O. Chua

Memorandum No. UCB/ERL M93/17

15 January 1993

**TWO-PARAMETER STUDY OF TRANSITION  
TO CHAOS IN CHUA'S CIRCUIT:  
RENORMALIZATION GROUP, UNIVERSALITY  
AND SCALING**

by

A. P. Kuznetsov, S. P. Kuznetsov, I. R. Sataev,  
and L. O. Chua

Memorandum No. UCB/ERL M93/17

15 January 1993

**ELECTRONICS RESEARCH LABORATORY**

College of Engineering  
University of California, Berkeley  
94720

**TWO-PARAMETER STUDY OF TRANSITION  
TO CHAOS IN CHUA'S CIRCUIT:  
RENORMALIZATION GROUP, UNIVERSALITY  
AND SCALING**

by

A. P. Kuznetsov, S. P. Kuznetsov, I. R. Sataev,  
and L. O. Chua

Memorandum No. UCB/ERL M93/17

15 January 1993

**ELECTRONICS RESEARCH LABORATORY**

College of Engineering  
University of California, Berkeley  
94720

**TWO-PARAMETER STUDY OF TRANSITION TO CHAOS IN CHUA'S CIRCUIT:  
RENORMALIZATION GROUP, UNIVERSALITY AND SCALING**

A. P. KUZNETSOV, S. P. KUZNETSOV, I. R. SATAEV

*Institute of Radio-engineering and Electronics, Russian Academy of Sciences,  
Zelenaja 38, Saratov, 410019, Russia*

and

L. O. CHUA

*Department of Electrical Engineering and Computer Sciences, University of  
California, Berkeley, CA 94720, USA*

A complex fine structure in the topography of regions of different dynamical behavior near the onset of chaos is investigated in a parameter plane of the 1-D Chua's map, which describes approximately the dynamics of Chua's circuit. Besides piecewise-smooth Feigenbaum critical lines, the boundary of chaos contains an infinite set of codimension-two critical points, which may be coded by itineraries on a binary tree. Renormalization group analysis is applied which is a generalization of Feigenbaum's theory for codimension-two critical points. Multicolor high-resolution maps of the parameter plane show that in regions nearby critical points having periodic codes, the infinitely intricate topography of the parameter plane reveals a property of self-similarity.

## 1. Introduction

In the usual scenarios of transition to chaos, one has in mind a sequence of bifurcations which is observed as one tunes a control parameter of a nonlinear system from a regime of regular dynamics to a chaotic one. However, in physics, engineering and other fields we often deal with systems controlled not by one but two or more essential parameters. In such cases instead of looking for a "scenario" we must pose a broader question concerning the global geometry of the parameter-space topography near the onset of chaos. Empirical data tell us that this topography can be extremely complicated and has a fractal-like structure. In Fig. 1 we show how it looks in a two-dimensional parameter space of Chua's circuit [Chua et al., 1986, Komuro et al., 1991]. This picture was made from the approximate 1-D Chua's map [Chua et al., 1986, Genot, 1993], and appears to give a remarkably good correspondence with that obtained from an exact description via the differential equations.

In Fig. 1 (a) different colors designate regions of periodic behavior with different periods while the black color corresponds to chaos, or periodic orbits having very high periods. There exist many cusps near the onset of chaos, and each cusp gives rise to a pair of emanating fold lines which coincide with the lines of tangent bifurcations. The presence of cusps and folds leads to the appearance of *multistability*: in the parameter region between each pair of folds the system exhibits at least two attractors having different basins of attraction in the state space. Narrow bands of periodicity are located along the fold lines and penetrate far into the area occupied by chaos. Also one can see lines of period-doubling bifurcations in the parameter plane. They converge to *critical lines*, which are just the piecewise-smooth parts of the boundary of chaos. To avoid clutter, Fig.1 (b) identifies the important boundary lines which will be referred to in this paper.

Suppose we draw an arbitrary one-parameter curve in the parameter plane of Fig.1 which starts from a region of regularity to a region of chaos. In a typical case it will cross transversely a critical line and, of course, the period-doubling lines which accumulate to it. This means that if we tune only one parameter in Chua's circuit and observe a transition to chaos we will see typically a classic period-doubling cascade. It is well known that this cascade exhibits a remarkable property of quantitative universality discovered by Feigenbaum and explained by him using a renormalization group (RG) analysis [Feigenbaum, 1978, 1979]. In particular, the bifurcation diagram near the critical lines exhibits a property of *self-similarity* or *scaling*. Namely, an interval encompassing regions of different dynamical regimes reproduces itself under a change in scale by the universal Feigenbaum's factor  $\delta=4.6692\dots$ , along any direction transversal to the critical line. Note, that this property is true in an *asymptotic* sense: it gives an increasingly higher precision as one explores a decreasingly narrower vicinity of the critical line.

If we turn to a two-parameter study, we can no longer restrict ourselves to the Feigenbaum scenario, which is a codimension-one bifurcation phenomenon, but must attempt to understand the nature of the entire boundary of chaos in Fig. 1. In this connection, it is crucial to note that the 1-D Chua's map happens to be *bimodal* in the parameter region under investigation. This means that the 1-D Chua's map has both a maximum and a minimum on an interval which is mapped onto itself. This is precisely the condition which is responsible for the complicated structure of the boundary of chaos. We shall show that beside the Feigenbaum critical lines, the boundary of chaos in the 1-D Chua's map (as well as in other bimodal maps, see Shell et al.[1983], MacKay & Tresser [1987,1988], Gambaudo et al. [1987], MacKay & van Zeijts [1988]) contains an infinite number of *codimension-two critical points*. In

Fig. 1(c) we show only a few of these points in the parameter plane. Hence, to uncover the nature of the entire boundary of chaos we must investigate the dynamics near these points.

We shall see that all possible types of codimension-two critical points are defined by a set of infinite binary codes. Among them the subset of codes having periodic tails is of particular importance. The topography of the parameter plane near the corresponding critical points reveals a property of *two-parameter self-similarity* or *vector scaling*: a two-dimensional structure of regions of different behavior is reproduced under a scale change along appropriate axes in the parameter plane. These self-similar two-dimensional patterns of the parameter space topography are *universal* for all bimodal maps (up to a linear parameter change) and depend only on the code of the associated critical point.

This paper is organized as follows. In Sec. 2 we recall the differential equations which modeled Chua's circuit and the basis for its reduction to a one-dimensional map. We also describe and explain how the shape of this map is changed as we vary two control parameters. The elegant construction of a binary tree of superstable orbits due to Shell et al. [1983] is reproduced for the 1-D Chua's map in Sec. 3. This construction allows us to find the location of codimension-two critical points which appear as end points of the tree branches in the limit of infinite branchings. Natural codes for the itineraries on the binary tree are introduced, which give also a coding rule for the critical points. In Sec. 4 we consider the solutions of Feigenbaum's RG equation corresponding to codimension-two critical points and apply them to analyze the dynamics of the 1-D Chua's map exactly at these points. We discuss the Cantor-like structure of critical attractors and their dimensions, the  $f(\alpha)$ -spectra and the Fourier spectra of corresponding dynamical regimes. Section 5 is devoted to the consideration of small perturbations

of the RG equation solutions which allows us to understand the universality and scaling properties of the parameter plane topography near the critical points. We present multi-color high-resolution computer graphics of two-dimensional patterns of the universal topography. Section 6 contains the conclusion and a brief discussion.

## 2. Chua's circuit and 1-D Chua's map

Chua's circuit is an electronic system modeled by the following set of differential equations

$$\dot{x} = \alpha(y-h(x)), \dot{y} = x-y+z, \dot{z} = -\beta y, \quad (1)$$

where  $x$ ,  $y$ ,  $z$  are the dynamical variables,  $\alpha$  and  $\beta$  are parameters, and  $h(x)$  is a piecewise-linear function which is chosen in accordance with Chua et al. [1986] as follows

$$\begin{aligned} h(x) &= (2x-3)/7, & x \geq 1 \\ &= -x/7, & |x| < 1 \\ &= (2x+3)/7, & x \leq -1 \end{aligned} \quad (2)$$

Using the Poincare section technique, the exact description of the system (1) may be reduced to a two-dimensional map which, in turn, may be approximated by a one-dimensional map

$$\pi^*: \quad X \Rightarrow \pi^*(X),$$

generally called *the Chua's map* in the literature. The procedure for constructing this map is described in detail by Chua et al. [1986] and Genot [1993].

Equations (2) and, consequently, the Chua's map depend on two parameters  $\alpha$  and  $\beta$ . However, in order to obtain clearer color graphics in a narrow region crammed with a very diverse structure, we have used the transformed parameters  $\alpha' = \alpha - 0.68\beta$  and  $\beta$  in Fig. 1, and in the following consideration.

Unfortunately, Chua's map does not have a simple explicit analytical representation. To compensate for this, we present in Fig. 2 a set of plots showing the shape of the map for a range of parameter values which cover the region of the

parameter plane depicted in Fig. 1. Observe that in some pictures the map is *bimodal*, i.e. it has both a maximum and a minimum point in the region of interest. We shall see that this leads to the appearance of complicated structures near the borderline of chaos.

### 3. Binary tree of superstable orbits

In our following consideration, the double superstable period- $2^n$  cycles will be of particular significance. They are defined as cycles which exist at some exceptional points of the parameter plane and which contain both extrema of the 1-D map in their orbits. The double superstable cycle will henceforth be referred to as a  $(p, q)$ -type cycle if the point of maximum is mapped into the point of minimum after  $p$  iterations and the minimum is mapped into the maximum after  $q$  iterations. The period of such a cycle is therefore equal to  $p + q$ .

Figure 3a (left most inset) shows an iteration diagram for Chua's map at the point of the parameter plane where a (1,1)-type double-superstable cycle of period 2 is realized. Starting from this point in the parameter plane let us move along a curve, at which any point satisfies the condition that the maximum is mapped into the minimum after one iteration. We will denote this curve by  $U(1)$ . Moving along the  $U(1)$  curve from the (1,1)-cycle we can find a point, where the minimum is mapped into the maximum again, but after three iterations. Hence, a period-4 double superstable cycle of type (1,3) exists here (see the inset in Fig. 3b). Alternatively, we can move from the initial (1,1)-cycle along another curve, denoting by  $D(1)$ , where the minimum is mapped into the maximum after one iteration. Along the  $D(1)$  curve, we can find a point where a period-4 double-superstable cycle exists which has the type (3,1) (see the inset in Fig. 3c). Note that our choice of the symbols " $U$ " and " $D$ " stands for "up" and "down", respectively.

In a similar manner we can start from any  $(p, q)$ -type double superstable cycle

of period  $p + q = 2^n$ . Then two curves,  $U(p)$  and  $D(q)$  emanate from the corresponding point in the parameter plane. The  $U(p)$  curve is defined by the condition that the maximum is mapped into the minimum after  $p$  iterations, and the  $D(q)$  curve is defined by the condition that the minimum is mapped into the maximum after  $q$  iterations. Moving along the  $U(p)$  (or  $D(q)$ ) curve we come to a point where a  $(p, p+2q)$ -type (or  $(2p+q, q)$ -type) period- $2^{n+1}$  double superstable cycle exists. We can depict the infinite family of  $U$  and  $D$  curves by drawing a *binary tree* as shown schematically in Fig.4. Note that the branching points correspond to double superstable cycles.

We shall restrict our following considerations to the upper half of the full binary tree. On this part of the tree the orbits of the Chua's map visit only two of the three piecewise-linear regions of the vector field (1). In Table 1 we give the coordinates of all branching points (i.e the location of double superstable cycles) up to period 64. Figure 5 shows the actually calculated configuration of the binary tree in the parameter plane of the Chua's map. In this picture we see how the branches of the tree enter into the complicated topological structure of Fig. 1.

Using the above notations, we can code each double superstable cycle naturally by a *finite* string of symbols  $U$  and  $D$ . Such a code designates a unique sequence of  $U$  and  $D$  curves in the parameter plane leading to this cycle from the initial point which corresponds to the  $(1, 1)$ -type cycle. Moving along the branches of the binary tree according to any given  $UD$ -code and tracing the corresponding attractor of the system we see a period-doubling cascade. At each branching point the attractor becomes a double superstable cycle of some period  $2^n$ . An *infinite* string of symbols  $U$  and  $D$  we can associate with an infinite period-doubling cascade observing when we move along the corresponding branches on the binary tree. Henceforth, the limit point of this cascade will be referred to as *a codimension-two critical point associated with the given infinite UD-code*, or simply *a critical point*. Note that

the period-doubling cascade under consideration here does *not* obey Feigenbaum's law; its convergence rate differs from Feigenbaum's and depends on the structure of the *UD*-code. In Table 2 we present the coordinates of some particular critical points generated by simple periodic *UD*-codes (see also Fig. 1 c). They are calculated with high precision using the method described in the Appendix A.

If we consider all possible combinations of infinite *UD*-codes, we would obtain an infinite number of critical points. The rough schematic sketch of the binary tree in Fig.4 shows their relative locations in the parameter plane. In fact, the set of codimension-two critical points forms a Cantor-like set of the points at the boundary of chaos. The remaining part of the boundary is formed by Feigenbaum's critical lines and does not require a special investigation.

#### 4. Dynamics of Chua's map at codimension-two critical points

In this section we will present a two-parameter generalization of Feigenbaum's theory for describing the dynamics of Chua's map at codimension-two critical points (see also Kuznetsov et. al [1993]). As much as possible, we explain the main ideas of the RG analysis via a more popular and intuitive approach. For a rigorous formulation we refer the reader to a number of works devoted to the development of theory of bimodal 1-D map from mathematical point of view (see MacKay & Tresser [1987,1988], Gambaudo et al. [1987], MacKay & van Zeijts [1988]).

##### 4.1. Renormalization group analysis

Let us take the point  $X = X^*$  at which the Chua's map has a maximum as our reference point and consider further the translated map  $f(x) = \pi^*(x + X^*) - X^*$  (see Fig.6 a, b). Let us apply this mapping twice (Fig. 6 c) and rescale the dynamical variable to normalize the resulting map  $f_1$  at the origin, namely,  $f_1(0) = 1$ . Then we obtain a new function  $f_1(x) = \alpha_1 f(f(x/\alpha_1))$ ,  $\alpha_1 = 1/f(f(0))$  (Fig. 6 d). A multiple repetition of this

procedure leads to a recurrent functional equation

$$f_{n+1}(x) = \alpha_n f_n(f_n(x/\alpha_n)), \quad (3)$$

where  $\alpha_n = 1/f_n(f_n(0))$ . This is just the RG equation considered at first by Feigenbaum [1978, 1979].

The above construction may seem rather abstract, but it really makes a lot of sense. A function  $f_n$  obtained by an  $n$ -fold iteration of Eq.(3) becomes a function which expresses the value of  $x$  after  $2^n$ -fold iterations of the Chua's map except for a change of scale in the variable  $x$ . This scale change is desirable because the interval of  $x$  which is essential for our consideration is expanded to cover the unit interval. In particular, it gives us the possibility to compare recursively the functions  $f_n$  with different  $n$  over the same unit interval. It follows from Eq.(3), that the functions  $f_n$  may be calculated via the rule

$$f_n(x) = f^{2^n}(x \cdot f^{2^n}(0)) / f^{2^n}(0), \quad (4)$$

where  $f^{2^n}(x)$  designates the  $2^n$ -fold functional composition of the map  $f(x)$ .

Thus, roughly speaking, the RG approach involves the construction and consideration of a sequence of maps (or evolution operators) which describe the dynamics over an exponentially increasing "time". (Here, we abused our terminology in using "time" to mean "number of iterations of the original map  $f(x)$ ".) In fact, the "time" intervals are doubled after each step of the RG transformation (3). This explains the efficiency of the RG approach near the onset of chaos. Indeed, it is here where the long-period behavior of the system is of particular importance.

Let us take now a critical point of Chua's map corresponding to a specific *UD*-code and make calculations according to Eq.(4) to obtain a sequence of  $f_n$  functions. Here we will observe a simple correlation. If the code has a  $k$ -periodic tail (i.e. a combination of  $k$  symbols begins to repeat after some position in the *UD*-code), then the sequence  $f_n$  also becomes  $k$ -periodic for a sufficiently large  $n$  (see the examples

in Fig. 7 a-c). Hence, the solution of the RG equation at this critical point converges to a period- $k$  cycle, which we called an *RG-cycle*. In particular, for  $k = 1$  the period is equal to unity and we have a *fixed point* of the RG equation. If the code is given by a random *UD*-sequence, then the sequence of  $f_n$  functions will appear to be chaotic (see the example in Fig. 7 d). In this case we say that an *RG-chaos* is realized.

Let us consider in detail the case of periodic solutions, i. e. fixed points and RG-cycles. To find an element of a period- $k$  RG-cycle means to find a function  $g(x)$  such that it is a fixed point of the  $k$ -fold iterated version of Eq.(3):

$$f_{n+k}(x) = \alpha_n^{(k)} f_n^{2^k}(x/\alpha_n^{(k)}). \quad (5)$$

Here  $\alpha_n^{(k)} = 1/f_n^{2^k}(0) = \prod_{i=0}^{2^k-1} \alpha_{n+i}$ , and  $f_n^{2^k}$  denotes the  $2^k$ -fold functional composition of the  $f$  map. In other words,  $g(x)$  must be a solution of the functional equation

$$g(x) = \alpha g^{2^k}(x/\alpha), \quad (6)$$

where  $\alpha = 1/g(g(0))$  is the value of the scaling factor  $\alpha_n^{(k)}$  at the fixed point of the RG equation. We remark that for a period- $k$  *RG-cycle*, Eq.(5) will have  $k$  fixed points, each obeying Eq.(6). However, it is sufficient to find *only one* of them because the remaining  $k - 1$  functions corresponding to elements of the *RG-cycle* can be obtained by 1, 2, ...,  $k-1$  direct iterations of the first fixed point function using Eq.(3).

Note that the solutions of Eq.(6) can be found without any reference to the nature of the initial map  $f(x)$ . This justifies our calling such solutions as *universal functions*. To find these functions with any prescribed precision it is convenient to use a polynomial approximation. Then Eq.(6) is reduced to a finite set of nonlinear algebraic equations involving the unknown polynomial coefficients. We solved this set of equations numerically by Newton's method. As our initial

approximation, the functions  $f_n$  were obtained from Eq.(4) by iterations of the Chua's map. The result of our calculations, i.e. the scaling constants  $\alpha$  and the coefficients of the polynomial expansions, are presented in Tables 3 and 4 for three simple critical points described by codes of period 1, 2 and 3, respectively. We show the plots of the universal functions in Fig. 8. Observe that they are in excellent agreement with the corresponding  $f_n$  functions from Fig. 7.

The period-1 codes  $UUUUUU\dots$  and  $DDDDDD\dots$  relate to the so-called *tricritical points*. Such points were introduced by Chang et al. [1981] while studying the two-parameter quartic map  $x_{n+1} = 1 + Ax_n^2 + Bx_n^4$ . For the code  $UUUUUU\dots$  the fixed point solution of the RG equation (Table 4) is the universal function  $g_T(x)$  evaluated by Chang et al. For the code  $DDDDDD\dots$  a different solution  $g_T^*(x)$  will be obtained. However it is connected with  $g_T(x)$  via a change of variable; namely,  $g_T^*(x)=[g_T(x^{1/2})]^2$ . The function  $g_T(x)$  may also be obtained in this case, but the origin must be taken at the minimum point of the  $\pi^*(X)$  map rather than at the maximum. Consequently, we need not distinguish these two cases of critical behavior.

Observe that there is an infinite number of tricritical points in the parameter plane of Chua's map because the corresponding codes may have an initial segment of *arbitrary* length and structure, followed by a tail of a repeating symbol  $U$ , or  $D$ , symbols. Some tricritical points are identified by circles in Figs. 1(c) and 4. Note that the locations of the tricritical points is quite specific: they all lie near the edges of the complicated parts of the boundary of chaos, and at the ends of the Feigenbaum's critical lines [Chang et al., 1981]. These properties justify the choice of the term "tricritical" because in the phase transition theory a point is called tricritical if an arbitrarily small neighborhood of this point contains phase transition lines of both the first and the second order. In our case the second-order phase transitions are associated with Feigenbaum's critical lines, while the

first-order phase transitions are associated with *jumps* observed at the fold lines. Indeed, both of them are present near each tricritical point.

When we discussed tricritical points, we have made the observation that the solution of the RG equation remains invariant under an interchange of the symbols  $U$  and  $D$  in the coding sequence, while simultaneously taking the other extremum as the origin. This kind of symmetry is valid for all codes. It follows from the observation that the maximum and the minimum play an identical role in the dynamics of the bimodal map. In particular, this symmetry leads to the appearance of an interesting property in the case of codes which reproduce themselves under a "shift" operation after interchanging the  $U$  and  $D$  symbols. For example, the period-2 code  $UDUDUD\dots$  and the period-4 code  $UUDDUUDD\dots$  have such a property. For these codes similar dynamical behaviors are observed not only after  $k$  steps of the RG transformation, but after  $k/2$  steps. We can say that the "period of the scaling-cycle" (i.e. the number of period doublings needed to reproduce the dynamics) is twice less than the period of the  $RG$ -cycle for this class of codes (for other codes they coincide).

We can take into account the observed symmetry by changing the coding rule. Namely, for each  $UD$ -sequence we construct an  $SC$ -sequence in the following manner: beginning from the second symbol of the  $UD$ -code, we write an "S" if the preceding symbol is the *same*, and a "C" if it is *changed*. For example, given the code  $UUDUDUUDDDDUDUD$ , we obtain the transformed code  $SCCCCSCSSCCCC\dots$ . The period of such an  $SC$ -sequence always coincides with the period of the "scaling-cycle". In the work by MacKay & van Zeijts [1988] a theory of bimodal 1-D maps based on the last coding rule is developed. However, their study involves two-component RG equations. So, this approach appears to be more complicated than the familiar Feigenbaum's analysis which we have adopted in this paper.

## 4.2. Properties of critical dynamics

Here we consider the dynamics of the Chua's map at codimension-two critical points with simple codes of period 1, 2 and 3. For comparison, we also present analogous results for the Feigenbaum's case by taking a representative point on a Feigenbaum's critical line in the parameter plane.

In Fig. 9 iteration diagrams are presented for the attractors of Chua's map corresponding to different critical points. In each picture four fragments having increasing levels of magnification are shown. Note that the magnification coefficient is chosen to be equal to the corresponding scaling factor  $\alpha$  obtained from the RG analysis (see Table 3). Reproduction of the same visible structure at different levels of resolution clearly demonstrates the local self-similarity of the attractors near an extremum of Chua's map. We see that on the boundary of chaos (including Feigenbaum's critical lines and codimension-two critical points) an attractor of the bimodal map appears to be a fractal set resembling the Cantor set but with a more complicated construction rule. In Appendix B we describe a procedure of approximating these sets by unions of an increasing number of intervals. In Fig. 10 we show several levels of this algorithm which is analogous to the well-known the Cantor set construction procedure.

To characterize quantitatively the global fractal structure of the critical attractors we appeal to a *multi-fractal* or *thermodynamic formalism* [Halsey et al., 1986, Vul et al., 1984].

To find the *Hausdorff dimension* of an attractor corresponding to a critical point having a  $k$ -periodic *UD*-code, we calculate the sums

$$S_n = \sum_{i=1}^{2^{n-1}} l_i^D, \quad (7)$$

where  $l_i$  denotes the length of the  $i$ -th interval in the  $n$ -th level of the attractor

approximation (Fig. 10). Then we take two levels,  $n$  and  $n + k$ , and choose  $D$  to make both sums  $S_n$  and  $S_{n+k}$  equal. The number  $D$  gives an approximate value for the Hausdorff dimension. It converges rather fast as  $n$  increases (see Table 5). The calculated Hausdorff dimension is a fraction and depends on the type of the critical point.

To obtain the  $f(\alpha)$ -spectra and the spectra of generalized dimensions  $D(q)$ , let us define the so-called partition functions  $\Gamma_n$  which depend on two parameters,  $q$  and  $\tau$ ,

$$\Gamma_n(q, \tau) = \sum_{i=1}^{2^{n-1}} p_i^q / l_i^\tau, \quad (8)$$

where  $p = 2^{-n}$  is a probabilistic measure attributed to each of the intervals  $l_i$  at the  $n$ -th level of the approximating attractor. Further, for any given  $\tau$  we choose  $q$  to make  $\Gamma_n$  and  $\Gamma_{n+k}$  equal to each other, thereby giving us a  $q(\tau)$  dependence. Using this  $q(\tau)$  function we can calculate

$$\alpha = (dq/d\tau)^{-1}, \quad f = \alpha q - \tau, \quad D(q) = \tau / (1 - q). \quad (9)$$

Now choosing  $q$  as a parameter we obtain the  $f(\alpha)$  and  $D(q)$  functions, which give us the  $f(\alpha)$ -spectrum and the generalized dimension spectrum at the  $n$ -th level. Then we increase  $n$  until the desired precision is attained. Figures 11 and 12 give the  $f(\alpha)$  spectra and  $D(q)$  spectra corresponding to four different critical points. Note that the maximum values of the  $f(\alpha)$  functions are equal to the Hausdorff dimensions of the attractors, that is  $D(0)$ . Moreover, the values of  $D(1)$  and  $D(2)$  are equal to the information dimensions and the correlation dimensions, respectively.

Figure 13 gives the Fourier spectra for the time series generated by Chua's map from different critical points. Qualitatively, all of these spectra have the same structure as the familiar Feigenbaum's spectrum (see Fig. 13 a). They all exhibit an infinite number of subharmonics with frequencies  $\omega \propto 2^{-n}$  and have a hierarchical organization: each  $n$ -th subharmonic level has less amplitude than the previous one.

However, the quantitative relations between the levels are different for each type of criticality.

## 5. Investigation of the parameter plane structure near critical points

Consider any critical point  $(\alpha_c, \beta_c)$  and make a small displacement in the parameter plane; namely,  $\alpha \Rightarrow \alpha_c + \Delta\alpha$ ,  $\beta \Rightarrow \beta_c + \Delta\beta$ . Clearly, the function  $f(x)$  which describes Chua's map will undergo a corresponding small perturbation. Thus, to investigate the dynamics in the neighborhood of critical points we have to deal with the perturbed solutions of the RG equation (3).

### 5.1. Linearized renormalization group equation

Here we shall study only perturbations of *periodic* solutions of the RG equation (3) because it will lead to a discovery of self-similar patterns in the parameter plane. However, if we have a period- $k$  solution, it will be more convenient to use Eq.(5). Here we shall introduce a little trick which does not change the final results but will simplify our calculations considerably. Let us redefine the RG transformation using the scaling factor  $\alpha$  corresponding to the critical point, instead of the factors  $\alpha_n^{(k)}$  which depend on  $n$ . Let us therefore search for the perturbed solutions of the equation

$$f_{n+k}(x) = \alpha f_n^{2^k}(x/\alpha), \quad (10)$$

rather than Eq.(5). Let us substitute  $f_n(x) = g(x) + \varepsilon h_n(x)$ ,  $\varepsilon \ll 1$ , and obtain the linear approximation

$$h_{n+k}(x) = \alpha [F_0^{N-1}(x)h_n(x/\alpha) + \sum_{m=1}^{N-2} F_m^{N-1}(x)h_n(g^m(x/\alpha)) + h_n(g^{N-1}(x/\alpha))], \quad (11)$$

where

$$F_m^{N-1}(x) = \left[ \frac{d}{d\xi} (g^{N-m}(\xi)) \right]_{\xi=g^{m+1}(x/\alpha)}, \quad N=2^k.$$

Equation (11) has the structure  $h_{n+1}(x) = \hat{M} h_n$ , where  $\hat{M}$  is a linear operator. If the perturbation  $h_0(x)$  contains a contribution from some eigenvector with eigenvalue  $\delta$ , then after  $p$ -fold iterations of (11) this contribution will be multiplied by the factor  $\delta^p$ . Hence, only those contributions that come from the eigenvectors having eigenvalues with modulus exceeding unity will survive under multiple RG transformations. For any *UD*-code there are two such essential eigenvectors which we denote by  $h_1(x)$  and  $h_2(x)$ . After several iterations of the RG transformation we obtain

$$h_{n+pk}(x) = C_1 \delta_1^p h_1(x) + C_2 \delta_2^p h_2(x) \quad (12)$$

where *only* the coefficients  $C_1$  and  $C_2$  depend on the initial perturbation  $h_0(x)$ .

The last relation leads us to the following important conclusions.

We see that the form of the evolution operator over long periods depends only on the two parameters  $C_1$  and  $C_2$ , which are the coefficients at the relevant eigenvectors. Hence, only these two parameters will determine the type of the dynamical behavior which result from a small initial perturbation of the map. *We can use the values of  $C_1$  and  $C_2$  as new coordinates in a parameter plane.* Because we consider only *small* perturbations, the values of  $C_1$  and  $C_2$  are related to the perturbations  $\Delta\alpha$  and  $\Delta\beta$  of the physical parameters by a *linear* transformation. Hence, if we choose appropriate coordinates, namely,  $(C_1, C_2)$ , we will see the same pattern of topography in the neighborhood of a codimension-two critical point with a particular *UD*-code for any bimodal one-dimensional map. This is *universality*.

Moreover, if we rescale  $C_1 \Rightarrow C_1/\delta_1^k$ ,  $C_2 \Rightarrow C_2/\delta_2^k$ , and increase  $n \Rightarrow n + k$  then we see from Eq. (12) that the evolution operator remains invariant. This means that the pattern of topography reproduces itself under the above change in scale when accompanied by an increase in the iteration number of the original map by a factor of  $2^k$ . Thus, this pattern is reproduced *ad infinitum* in smaller and smaller

neighborhoods of the critical point. This is precisely the property of *self-similarity* or *scaling*. Henceforth, we will call  $(C_1, C_2)$  the *scaling coordinates*.

Recall that to obtain the above formulations we have used Eq. (12) which was based on the assumption that only two terms survive. This assumption is strictly valid only in an asymptotic sense, i.e. as  $n \Rightarrow \infty$ . In other words, the universality and scaling properties hold, rigorously speaking, only in a sufficiently small neighborhood of a critical point. However, we shall see that in practice, this restriction is not very strong.

We have to make a particular remark concerning the *symmetrical* codes mentioned at the end of subsection 4.1. If the code reproduces itself after a shift and a change of symbols  $U \Leftrightarrow D$ , then the pattern of topography is reproduced *not only* after a change in scale by factors  $\delta_1$  and  $\delta_2$ , but also by the square roots of  $\delta_1$  and  $\delta_2$ . In this case the characteristic time of the dynamical regimes is multiplied by  $2^{k/2}$  instead of  $2^k$ .

To find the relevant eigenvectors  $h_{1,2}(x)$  and the eigenvalues  $\delta_{1,2}$  we again use polynomial approximation to obtain a finite set of algebraic equations instead of the RG equation in function space. Hence, we have reduced the infinite-dimensional eigenproblem for the linear operator (11) to a finite-dimensional eigenproblem. The eigenvalues for several types of critical points calculated by this method are given in Table 3.

## 5.2. Self-similarity and topography of parameter space near codimension-two critical points

To demonstrate the above properties of the parameter plane near codimension-two critical points we need, at first, to find a connection between the physical parameters  $\alpha$  and  $\beta$  of Chua's map, and the scaling coordinates  $C_1$  and  $C_2$ . A special

procedure for this purpose has been developed (see Appendix C). As a result we obtain the following relations for three critical-point representatives:

$$1) \text{ Tricritical point } UUUUUU\dots, \alpha_c = 3.4264643, \beta_c = 4.1192463, \\ \alpha - \alpha_c = 0.54 C_1 + 0.67 C_2, \quad \beta - \beta_c = 0.83 C_1 + 1.00 C_2. \quad (13)$$

$$2) \text{ Period-2 point } UDUDUD\dots, \alpha_c = 3.3905335, \beta_c = 4.0549327, \\ \alpha - \alpha_c = -0.45 C_1 + 0.57 C_2, \quad \beta - \beta_c = -0.71 C_1 + 0.86 C_2. \quad (14)$$

$$3) \text{ Period-3 point } UUDUUD\dots, \alpha_c = 3.47250666, \beta_c = 4.18643549, \\ \alpha - \alpha_c = -0.51 C_1 + 0.65 C_2, \quad \beta - \beta_c = -0.80 C_1 + 0.98 C_2. \quad (15)$$

Figure 14 shows again a general view of the  $(\alpha', \beta)$  parameter plane of Chua's map. Chosen for detailed consideration are neighborhoods of the three critical points which are depicted as parallelograms formed by lines parallel to the  $C_1$  and  $C_2$  axes, respectively. In Figs. 15 - 17 the pictures inside these parallelograms are presented in terms of the scaling coordinates  $C_1$  and  $C_2$ . In each of these figures, a critical point is located exactly at the center of the picture. A small box is marked and shown on the right side after magnification. The magnification factors are chosen equal to the  $\delta_1$  and  $\delta_2$  - eigenvalues of the linearized RG operator corresponding to the critical point. Different colors denote periodic behavior with different periods; chaos or very high periodic orbits are denoted in black. To see more explicitly the similarity of the pictures we have redefined the colors in the magnified pictures. The legend is given in the figure captions.

Observe the remarkable reproduction of the topography inside the small rectangles, even through the initial neighborhoods of the critical points which we have chosen are not very small. Moreover, the topography of the neighborhood of the period-2 point  $UDUDUD\dots$  is also reproduced when we use the magnification factors  $(\delta_1^{1/2})$  and  $\delta_2^{1/2}$ , in view of the symmetry of the code.

## 6. Conclusion

In this paper we have discussed some peculiarities of the boundary of chaos in a parameter plane of Chua's circuit using the approximate 1-D Chua's map. We have emphasized the universality and scaling properties of two-dimensional patterns in the parameter plane topography. We have presented examples of such patterns for neighborhoods of several special points on the boundary of chaos. Our analysis represents a two-parameter analog of the familiar Feigenbaum's theory, which is valid only for typical one-parameter period-doubling cascades. Such generalizations have recently attracted much attention among theorists (see Chang et al. [1981], Shell et al. [1983], Fraser & Kapral [1984], Gambaudo et al. [1987], MacKay & Tresser [1987, 1988], MacKay & van Zeijts [1988], Carcasses et al. [1991]). However, in contrast to Feigenbaum's universality which has been observed in a large number of real systems, there has not been any physical experiments which confirmed the two-parameter universal phenomena near the onset of chaos. Although our work is also theoretical, our equations come from a concrete physical system; namely, Chua's circuit, which has many advantages from an experimental point of view. First of all, this system is easily built as a real electronic device. Secondly, the electronic nature of this system makes it easy to process and analyze generated signals, in sharp contrast to the severe difficulties encountered in experiments on hydrodynamics. Finally, this system admits a very accurate description by an approximate 1-D map, and this circumstance gives us the possibility for a detailed comparison between experiment and theory. We hope therefore that this paper will stimulate much experimental investigations in the direction we have suggested.

## Appendix

### A. High precision calculation of codimension-two critical points

When a period-doubling bifurcation occurs a new stable cycle of twice the period arises; the original cycle do not disappear but merely becomes unstable. Thus, corresponding to the accumulation points of the period-doubling cascades (including points of Feigenbaum's lines and codimension-two critical points) a bimodal map has a complete set of period- $2^n$  cycles, where  $n$  can be arbitrarily large. All these cycles are unstable. If we pick an element  $x$  of such a cycle, make a small perturbation  $\Delta x$  and look at how it changes after one period of the cycle, we see a corresponding change  $\mu\Delta x$ , where  $|\mu| > 1$ . The value  $\mu$  is called the *multiplier* of the cycle. If  $x_1, \dots, x_N$  are elements of a period- $N$  cycle of the 1-D map  $f(x)$ , then its multiplier is obtained by the chain rule

$$\mu = \prod_{i=1}^N f'(x_i). \quad (\text{A.1})$$

The multipliers of period- $2^n$  cycles corresponding to critical points possess the following property of universality:

Consider a point having a *UD*-code with a *period- $k$  tail*. Then for a sufficiently large  $n$ , the multipliers of period- $2^n$  cycles exhibit a *period- $k$  dependence on  $n$* ; they assume a definite set of  $k$  values  $\mu_c^{(1)}, \mu_c^{(2)}, \dots, \mu_c^{(k)}$ . These values are *universal* numbers intrinsic to the given  $k$ -periodic *UD*-sequence. (Note that the values of  $\mu_c^{(i)}$  for different  $i$  are not necessarily distinct: for symmetrical codes mentioned in subsections 4.1 and 5.2 the multipliers are repeated with a smaller period equal to  $k/2$ .)

The universal multipliers for a given critical point may be obtained via the corresponding solution of the RG equation (6) which we have denoted by  $g(x)$ . Indeed, as we have explained in Sec.4, this solution defines an evolution operator for large

$n$ 's which is universal up to a change in scale. However, the scale change does not influence multipliers. Hence, if we calculate the multipliers of the period-1, 2, ...,  $2^k$  cycles of the map  $g(x)$ , then we would obtain the  $\mu_c^{(i)}$  values. In Table 3 we give these values among other universal quantifiers for critical points with simple codes.

To find codimension-two critical points in the parameter plane we initially obtain a rather rough estimate of their positions as limit points of the corresponding itineraries on the binary tree. Then, choosing some number  $n$  we try to find such  $\alpha$  and  $\beta$  values to make both the multipliers of period- $2^n$  and  $2^{n+k}$  cycles equal to appropriate universal values. Then we increase  $n$  and repeat the procedure until a desired precision is attained. The results converge quickly with increasing  $n$ .

## **B. Constructing Cantor-like attractors at critical points**

The Cantor-like algorithm for constructing subsequent approximating sets of intervals is well known for the Feigenbaum's attractor. For example, for  $\beta = 10$  we find the Feigenbaum's critical point (i.e. the accumulation point of the period-doubling cascade) in the Chua's map at  $\alpha = \alpha_c = 6.5408510\dots$ , and the maximum is located at the point  $X^* = 1.1942673\dots$ . Taking  $X_0 = X^*$  we obtain  $X_1 = \pi^*(X_0) = 1.4353$ ,  $X_2 = \pi^*(X_1) = 1.0677$ ,  $X_3 = \pi^*(X_2) = 1.3830$ ,  $X_4 = \pi^*(X_3) = 1.2388$ ,  $X_5 = \pi^*(X_4) = 1.4271$ ,  $X_6 = \pi^*(X_5) = 1.1005$ ,  $X_7 = \pi^*(X_6) = 1.4054$ ,  $X_8 = \pi^*(X_7) = 1.1756\dots$

Then the attractor is approximated

by the interval  $[X_1, X_2]$  at the 1-st level of the construction,

by the union of two intervals  $[X_1, X_3]$  and  $[X_2, X_4]$  at the 2-nd level,

by the union of four intervals  $[X_1, X_5]$ ,  $[X_2, X_6]$ ,  $[X_3, X_7]$ , and  $[X_4, X_8]$  at the 3-d level.

At the  $n$ -th level, the attractor is approximated by a set  $A_n$  made up of the union of  $2^{n-1}$  intervals  $[X_1, X_{2^{n-1}+1}]$ ,  $[X_2, X_{2^{n-1}+2}]$ , ...  $[X_{2^{n-1}}, X_{2^n}]$ ; namely,

$$A_n = \bigcup_{i=1}^{2^{n-1}} [x_i, x_{i+2^{n-1}}] . \quad (\text{A.2})$$

Figure 10 (a) shows the first few levels of this construction.

To generalize the above rule let us recall our notation  $(p, q)$  for double superstable cycles (Sec.3). Consider a specific *UD*-code which gives the itinerary on the binary tree leading to a desired critical point. Following this itinerary, we obtain a sequence of integer pairs  $(p, q)_n$ , where  $p + q = 2^n$ . The integers  $n = 1, 2, 3, \dots$  will define again the level number. From the *bimodal* map we can calculate *two* sequences of iterations:  $y_i$  and  $z_j$ ,  $i, j = 1, 2, 3, \dots$ , starting from the maximum and the minimum, respectively. To obtain the end points of the set of intervals for approximating the attractor at the  $n$ -th level, we find a pair  $(p, q)_n$ , and take  $p$  terms from the first sequence, and  $q$  terms from the second sequence. Namely, we define

$$\begin{aligned} x_i &= y_i, \quad 1 \leq i \leq p, \\ z_{i-p}, & \quad p < i \leq p + q. \end{aligned} \quad (\text{A.3})$$

Substituting these  $x_i$  into Eq. (A.2) we obtain a set made of union of intervals which gives an  $n$ -th level approximation of the attractor.

Let us consider an example and choose a critical point with the period-2 code *UDUDUD*... having coordinates  $\alpha_c = 3.390533\dots$ ,  $\beta_c = 4.054932\dots$ (see Table 2). For these parameters the maximum and the minimum of the Chua's map are located at the points  $X^* = 1.2177503\dots$  and  $Y_0 = X^{**} = 1.4418532\dots$ , respectively. Taking  $Y_0 = X^*$  and  $Z_0 = X^{**}$ , we obtain two sequences:

$$\begin{aligned} Y_1 &= \pi^*(Y_0) = 1.4503, Y_2 = \pi^*(Y_0) = 1.1192, Y_3 = \pi^*(Y_0) = 1.4147, Y_4 = \pi^*(Y_0) = 1.1658, \\ Y_5 &= \pi^*(Y_0) = 1.4396, Y_6 = \pi^*(Y_0) = 1.0921, Y_7 = \pi^*(Y_0) = 1.3950, Y_8 = \pi^*(Y_0) = 1.2321, \dots \end{aligned}$$

and

$$Z_1 = \pi^*(Z_0) = 1.0909, Z_2 = \pi^*(Z_0) = 1.3940, Z_3 = \pi^*(Z_0) = 1.2351, Z_4 = \pi^*(Z_0) = 1.4489, \\ Z_5 = \pi^*(Z_0) = 1.1094, Z_6 = \pi^*(Z_0) = 1.4080, Z_7 = \pi^*(Z_0) = 1.1892, Z_8 = \pi^*(Z_0) = 1.4469, \dots$$

From Fig. 4 we see that the sequence of  $(p, q)$  pairs for the above critical point is given by  $(1,1), (1,3), (5,3), (5,11), (21, 11), \dots$  Hence, to obtain the sequence of values  $X_i$  which give the ends of the intervals approximating the attractor we must take

1 term from the first sequence and 1 from the second at the 1-st level;

1 term from the first sequence and 3 from the second at the 2-nd level;

5 terms from the first sequence and 3 from the second at the 3-d level;

5 term from the first sequence and 11 from the second at the 4-th level;

and so on.

For example, for the level number  $n=3$  we obtain:

$$X_1=1.4503, X_2=1.1192, X_3=1.4146, X_4=1.1658, X_5=1.4396, X_6=1.0909, X_7=1.3940, \\ X_8=1.2351, \text{ and the approximated attractor set is defined by the union of the intervals } [X_1, X_5], [X_2, X_6], [X_3, X_7], \text{ and } [X_4, X_8].$$

Figure 10 b, c, and d shows several levels of the attractor for some critical points of codimension two.

### C. Connection between physical and scaling coordinates in the parameter plane

Consider a critical point  $(\alpha_c, \beta_c)$  which has a  $UD$ -code with a period- $k$  tail. Let us take two left finite strings of  $UD$ -code containing  $n$  and  $n + k$  symbols. We can find the points  $(\alpha_1, \beta_1)$  and  $(\alpha_2, \beta_2)$  in the parameter plane, where the two corresponding double-superstable cycles exist; henceforth they are identified as *similar*.

It follows from the RG analysis that the coordinates of these points must be

related by some linear transformation

$$\begin{bmatrix} \Delta\alpha \\ \Delta\beta \end{bmatrix}_1 = \begin{bmatrix} A & B \\ C & D \end{bmatrix} \begin{bmatrix} \Delta\alpha \\ \Delta\beta \end{bmatrix}_2 \quad (\text{A.4})$$

where  $\Delta\alpha_{1,2} = \alpha_{1,2} - \alpha_c$ ,  $\Delta\beta_{1,2} = \beta_{1,2} - \beta_c$  and where the elements  $A, B, C, D$  are fixed for the critical point  $(\alpha_c, \beta_c)$ . If the scaling property holds with infinite precision, then the matrix  $\begin{bmatrix} A & B \\ C & D \end{bmatrix}$  would have eigenvalues  $\delta_1$  and  $\delta_2$  equal to those predicted from the RG analysis. It follows that

$$A + D = \delta_1 + \delta_2 \quad \text{and} \quad AD - BC = \delta_1 \delta_2. \quad (\text{A.5})$$

Hence, if we know the  $\alpha$  and  $\beta$  coordinates of the points corresponding to the two similar double-superstable cycles, we could find the four elements of the matrix from the four equations defined by (A.4) and (A.5).

However, in practice, this simple method does not yield a satisfactory precision because the scaling holds only approximately for a sufficiently large values of  $n$ . To improve this approach, we take coordinates not of one, but of *two* pairs of similar double-superstable cycles. The second pair is defined by the same two  $n$ - and  $n+k$ -symbol strings except for the *last* symbol. Their coordinates must obey Eq. (A.4) too. Hence, we obtain from (A.4) and (A.5) *eight* equations involving *four* unknown matrix elements. They can be evaluated by a least square method. Finally, we calculate eigenvectors of the matrices via the usual techniques. We have found this approach to give satisfactory precision. The numerical results for three critical points with simple codes are presented in Sec.5.

## References

- Carcasses, J., Mira, C., Bosch, M., Simo, C. & Tatjer, J.C. [1991] "Crossroad area - spring area transition (1) Parameter plane representation", *Int. J. Bifurc. & Chaos* **1**, 183-196.

- Chang, S.J., Wortis, M. & Wright, J.A. [1981] "Iterative properties of a one-dimensional quartic map. Critical lines and tricritical behavior", *Phys. Rev.* **A24**, 2669-2684.
- Chua, L.O., Komuro, M. & Matsumoto, T. [1986] "The double scroll family, Parts I and II", *IEEE Trans. Circuits and Systems* **CAS-33**, 1072-1118.
- Feigenbaum, M.J. [1978] "Quantitative universality for a class of nonlinear transformations", *J. Stat. Phys.* **19**, 25-52.
- Feigenbaum, M.J. [1979] "The universal metric properties of nonlinear transformations", *J. Stat. Phys.* **21**, 669-706.
- Fraser, S. & Kapral, R. [1984] "Universal vector scaling in one-dimensional maps", *Phys.Rev.* **A25**, 3223-3233.
- Gambaudo, J.M., Los, J.E. & Tresser, G. [1987] "A Horseshoe for the Doubling Operator Topological Dynamics for Metric Universality", *Phys.Lett.* **A123**, 60.
- Genot, M. [1993] "Application of 1-D Chua's map from Chua's circuit: A pictorial guide", *J. of Circuits, Systems & Computers* **3**, No 2.
- Komuro, M., Tokunaga, R., Matsumoto, T., Chua L. O. & Hotta A. [1991] "Global bifurcation analysis of the double scroll circuit", *Int. J. Bifurc. & Chaos* **1**, 139-182.

- Kuznetsov, A.P., Kuznetsov S.P., Sataev, I.R. & Chua, L.O. [1993] "Self-similarity and universality in Chua's circuit via the approximate Chua's 1-D map", *J. of Circuits, Systems & Computers* 3, No 2.
- MacKay, R.S. & Tresser, C. [1987] "Some flesh on the skeleton: The bifurcation structure of bimodal maps", *Physica D27*, No 3, 412-422.
- MacKay, R.S. & Tresser, C. [1988] "Boundary of topological chaos for bimodal maps of the interval", *J.London Math.Soc.* 37, No 1, 164-181.
- MacKey, R.S. & van Zeijts, J.B.J. [1988] "Period doubling for bimodal map: a horseshoe for a renormalization group operator", *Nonlinearity*, 1, No 1, 253-277.
- May, R.M. [1976] "Simple mathematical models with very complicated dynamics", *Nature* 261, No 6, 459-467.
- Myrberg, P.J. [1963] "Iteration der reelen polynome zweiten grades" *Ann. Acad. Sci. Fennica A336*, 1-18.
- Shell, M., Fraser, S. & Kapral, R. [1983] "Subharmonic bifurcations in the sine map: An infinite hierarchy of cusp bistabilities", *Phys.Rev.* A28, 373-379.
- Vul, E.B., Sinai, Ya.G. & Khanin, K.M. [1984] "Feigenbaum universality and the thermodynamic formalism", *Russian Math. Surveys* 39:3, 1-40.

Table 1. Coordinates of points corresponding to double-superstable cycles in the  $(\alpha, \beta)$  parameter plane of Chua's map

Period	Code	Type	$\alpha$	$\beta$
2	U	(1,1)	2.428631394	2.668405542
4	U	(1,3)	3.181220121	3.745645702
8	UU	(1,7)	3.385570546	4.056225192
	UD	(5,3)	3.304172652	3.924564694
16	UUU	(1,15)	3.420523839	4.110073977
	UUD	(9,7)	3.451202705	4.154022937
	UDD	(5,11)	3.371607421	4.026497755
	UDD	(13,3)	3.322086756	3.950706806
32	UUUU	(1,31)	3.425635489	4.117966453
	UUUD	(17,15)	3.446341076	4.148658902
	UUUD	(9,23)	3.468080765	4.179722569
	UUDD	(25,7)	3.460629330	4.168074575
	UUUU	(5,27)	3.381321925	4.041250484
	UUUD	(21,11)	3.384883151	4.046391549
	UUDD	(13,19)	3.347452437	3.988976155
	UUDD	(29,3)	3.324572114	3.954335126
64	UUUUU	(1,63)	3.426349800	4.119069717
	UUUUU	(33,31)	3.435019191	4.131995516
	UUUUU	(17,47)	3.450729549	4.155286007
	UUUUU	(49,15)	3.450159213	4.154362375
	UUUUU	(9,15)	3.470473747	4.183372220
	UUUUU	(9,55)	3.472615955	4.186547036
	UUUUU	(41,23)	3.466915690	4.177636557
	UUUUU	(57,7)	3.461930279	4.170013929
	UUUUU	(5,59)	3.382650546	4.043269477
	UUUUU	(37,27)	3.386207858	4.048583042
	UUUUU	(21,43)	3.389159747	4.052862761
	UUUUU	(53,11)	3.386774450	4.049225161
	UUUUU	(13,51)	3.351382924	3.994918392
	UUUUU	(45,19)	3.351198826	3.994606699
	UUUUU	(29,35)	3.333371880	3.967599998
	UUUUU	(61,3)	3.324913299	3.954833242

Table 2. Some critical points of the Chua's map

Type	Codes	$\alpha, \beta$	
Feigenbaum		6.54085103	10.00000000
Tricritical	<i>UUUUUUUUU...</i>	3.42646411	4.11924628
	<i>UUDDDDDDD...</i>	3.46213786	4.17032337
	<i>UDUUUUUUU...</i>	3.38286211	4.04359100
	<i>UDDDDDDDD...</i>	3.32496761	3.95491253
Period-2 RG cycle	<i>UDUDUDUDU...</i>	3.39053348	4.05493270
Period-3 RG cycle	<i>UUDUUDUUD...</i>	3.47250666	4.18643549
	<i>UDDUDDUDD...</i>	3.35238709	3.99639697

Table 3. Universal numbers for several types of critical points

	Feigenbaum	Tricritical	RG cycle 2	RG cycle 3
Codes		<i>...UUUUUU...</i>	<i>...UDUDUD...</i>	<i>...UUDUUD...</i>
Scaling factor $\alpha$	-2.502907876	-1.690302971	-4.862645091	8.030267587
Parameter scaling factors $\delta_1, \delta_2$	4.66920161	7.28468622 2.85712414	35.9286114 14.5957450	244.7687073 46.2910330
Critical multipliers $\mu$	-1.60119133	-2.05094049	-2.27516954 -2.27516954	-2.14347576 -2.25392276 -2.27787495

Table 4. Coefficients of polynomial approximation for  
 RG equation solutions  $g(x) = \sum c_v x^v$

Tricritical ...UUUUU...		Period-2 ...UDUDUD...		Period-3 ...UUDUUD...	
v		v		v	
0	1	0	1	0	1
4	-1.834107907	2	-2.659451025	2	-2.325802068
8	0.012962226	4	-0.457073109	4	-0.431810277
12	0.311901739	6	2.998999170	6	1.769729434
16	-0.062014652	8	-0.776220408	8	0.021283412
20	-0.037539287	10	-1.414948457	10	-0.743118612
24	0.017647313	12	1.370177562	12	0.209345906
28	0.001938265	14	-0.068984505	14	-0.012063820
32	-0.002820471	16	-0.580666023	16	0.679983089
36	0.000115457	18	0.174967752	18	-1.504391919
40	0.000399471	20	0.400482740	20	1.918087529
44	-0.000024793	22	-0.536278594	22	-1.799808881
48	-0.000121641	24	0.338283919	24	1.244301917
52	0.000070434	26	-0.126059065	26	-0.586942935
56	-0.000017980	28	0.026941179	28	0.166339351
60	0.000001909	30	-0.002582550	30	-0.021240090

Table 5. Evaluation of Hausdorff dimension for attractors  
 of Chua's map in different critical points

Feigenbaum		Tricritical		Period-2 RG-cycle		Period-3 RG-cycle	
Level	D	Level	D	Level	D	Level	D
2-3	0.536914	2-3	0.65432	2-4	0.60252	2-5	0.60262
3-4	0.538250	3-4	0.65327	3-5	0.62194	3-6	0.61440
4-5	0.538009	4-5	0.64744	4-6	0.61599	4-7	0.61631
5-6	0.538053	5-6	0.64535	5-7	0.61260	5-8	0.61497
6-7	0.538044	6-7	0.64382	6-8	0.61484	6-9	0.61664
7-8	0.538045	7-8	0.64327	7-9	0.61409	7-10	0.61585
8-9	0.538045	8-9	0.64310	8-10	0.61427		

## FIGURE CAPTIONS

Fig. 1. (a) Topography of the dynamical behavior of the 1-D Chua's map near the onset of chaos in the  $(\alpha', \beta)$  parameter plane,  $\alpha' = \alpha - 0.68\beta$ . At each of the 300x300 pixels a number of iterations were made and the presence of periodicity was checked. Different periods are coded by colors (1 - green, 2 - yellow, 4 - violet, 8- red, 3 - pink, 6 - light blue). Black corresponds to chaos or unrecognized long-period regimes.

(b) Sketch of the parameter plane identifying some important areas, lines and points: D1, D2, and D3 are the lines of the first, second and third period-doubling bifurcations, respectively, F denotes a Feigenbaum's critical line. Two (of an infinite number) cusps (C) and their associated pairs of fold lines are marked.

(c) Sketch of the parameter plane where the location of several codimension-two critical points is shown: tricritical points are marked by circles; the square and triangle denote critical points corresponding to RG cycles of period 2 and 3, respectively.

Fig. 2. Plots of the Chua's map  $X \Rightarrow X', X' = \pi^*(X)$  for a set of parameter values  $\alpha'$  and  $\beta$ . A diagonal line  $X = X'$  is also shown in each plot. The parameter region chosen corresponds approximately to the area near the boundary of chaos. Bimodality of Chua's map may be seen in some of the pictures.

Fig. 3. An illustration of the construction of a superstable orbit binary tree. The itineraries are coded by a sequence of symbols  $U$  (up) and  $D$  (down). The double superstable cycles from Chua's 1-D map correspond to the branching points of the binary tree. (a)  $\alpha=2.42863139$ ,  $\beta=2.66840554$ ; (b)  $\alpha=3.18121220$ ,  $\beta=3.74564570$ ; (c)  $\alpha=3.00564702$ ,  $\beta=3.41905639$ ; (d)  $\alpha=3.38557055$ ,  $\beta=4.05622519$ ; (e)  $\alpha=3.30417265$ ,  $\beta=3.92456469$ .

Fig. 4. Rough schematic sketch of the binary tree in the parameter plane. The branching points correspond to double superstable cycles; their  $(p, q)$ -types are shown. A codimension-two critical point is located at the end of every path through an infinite number of branching points. Since there are infinitely many distinct paths, it follows that there are infinitely many critical points. Each critical point is coded by an infinite sequence of symbols  $U$  and  $D$  according to the itinerary leading to these point along the branches labeled by  $U$  and  $D$ . Some of the

tricritical points are identified by solid circles (for the case when the tail of the code is ...UUUUU...) and by open ones (for the case when the tail of the code is ...DDDD...). The critical points corresponding to a period-2 (code UDUDUD...) and a period-3 (code UUDUUD...) cycle of the RG equation are identified by a small square and a small triangle and labeled RG2 and RG3, respectively. Pieces of Feigenbaum's critical lines (shown dotted) are labeled by F.

Fig. 5. Location of the binary tree in the  $(\alpha', \beta)$  parameter plane of Chua's map superimposed upon the background of the topography reproduced from Fig.1.

Fig.6. Plots of some maps which appear during the RG analysis of the Chua's map. For a specific example, the tricritical point  $\alpha=3.42646406$ ,  $\beta=4.11924620$  is chosen.

- (a) The original map  $\pi^*(x)$  at the critical point,
- (b) the translated map  $f(x) = \pi^*(x + X^*) - X^*$ ,
- (c) the double iterated map  $f(f(x))$ ,
- (d) the renormalized double iterated map  $f_1(x)$ .

Fig. 7. Graphs of functions from the sequence  $f_n(x)$  which were generated by iterating Eq.(3). Values of  $n$  are given for each function. The Chua's 1-D map was taken as the initial function  $f_0$ , the origin being chosen at the point of its maximum (see Fig.1), for the following parameter values:

- (a)  $\alpha=3.42646406$ ,  $\beta=4.11924620$ , code UUUUUU... This correspond to a fixed point of the RG equation.
- (b)  $\alpha=3.39053347$ ,  $\beta=4.05493268$ , code UDUDUD... This correspond to a period-2 cycle of the RG equation.
- (c)  $\alpha=3.47250666$ ,  $\beta=4.18643549$ , code UUDUUD... This correspond to a period-3 cycle of the RG equation.
- (d)  $\alpha=3.46837499$ ,  $\beta=4.17984652$ , code UUDDUDU...This correspond to renormalization chaos.

Fig. 8. Universal functions obtained via numerical solution of the RG equation at different critical points: (a) Feigenbaum's point, (b) tricritical point coded UUUUUU..., (c) period-2 critical point coded UDUDUD..., (d) period-3 critical point coded UUDUUD... For the cases (c) and (d) two and three functions are shown corresponding to all elements of the RG cycles.

Fig. 9. Iteration diagrams of Chua's map  $X \Rightarrow X'$ ,  $X' = \pi^*(X)$  for different critical points (see the  $\alpha$  and  $\beta$  coordinates in Table 2): (a) Feigenbaum's point, (b) tricritical point corresponding to the code  $UUUUUU\dots$ , (c) the period-2 critical point ( $UDUDUD\dots$ ), (d) the period-3 critical point corresponding to the code  $UUDUUD\dots$ . In each picture a fragment is selected and shown separately after several magnification steps. The respective factors of magnification  $\alpha$  are found from the RG analysis (see Table 3).

Fig. 10. Several subsequent steps in the construction of the Cantor-like attractors of the Chua's map at different critical points: (a) Feigenbaum's point, (b) tricritical point ( $UUUUUU\dots$ ), (c) period-2 critical point ( $UDUDUD\dots$ ), (d) period-3 critical point ( $UUDUUD\dots$ ).

Fig. 11.  $f(\alpha)$  spectra for critical attractors of the Chua's map: (a) Feigenbaum's point, (b) tricritical point ( $UUUUUU\dots$ ), (c) period-2 critical point ( $UDUDUD\dots$ ), (d) period-3 critical point ( $UUDUUD\dots$ ).

Fig. 12. Spectra of generalized dimensions for critical attractors of the Chua's map: (a) Feigenbaum's point, (b) tricritical point ( $UUUUUU\dots$ ), (c) period-2 critical point ( $UDUDUD\dots$ ), (d) period-3 critical point ( $UUDUUD\dots$ ).

Fig. 13. Fourier spectra for time series generated by Chua's map at the critical points: (a) Feigenbaum's point, (b) tricritical point ( $UUUUUU\dots$ ), (c) period-2 critical point ( $UDUDUD\dots$ ), (d) period-3 critical point ( $UUDUUD\dots$ ).

Fig. 14. Portions of the topography from Fig.1 selected for detailed consideration. Neighborhoods of the critical points are shown by parallelograms. A critical point is located in the center of each parallelogram: (1) tricritical point coded by  $UUUUUU\dots$ , (2) the critical point coded by  $UDUDUD\dots$ , (3) the critical point coded by  $UUDUUD\dots$ .

Fig. 15. The universal two-dimensional pattern of the parameter plane topography near the tricritical point  $UUUUUU\dots$  which is located in the center of the pictures. The picture on the left shows the interior of the parallelogram labeled "1" in Fig. 14. Scaling coordinates  $(C_1, C_2)$  are used here (see Eq.(13)). The picture on the right shows a small fragment after magnification by  $\delta_1$  and  $\delta_2$  along the vertical and

the horizontal axes, respectively. The following color codes are used. For the left picture: 2 - green, 4 - yellow, 8 - violet, 16- red, 6 - pink, 12 - light blue; for the right picture the same colors correspond to the doubled periods: 4 - green, 8 - yellow, 16 - violet, 32- red, 12 - pink, 24 - light blue.

Fig. 16. The universal two-dimensional pattern of the parameter plane topography near a critical point with the period-2 code  $UDUDUD\dots$ . The critical point is located in the center of the pictures. The picture on the left shows the interior of the parallelogram labeled "2" in Fig. 14. Scaling coordinates  $(C_1, C_2)$  are used here (see Eq.(14)). The picture on the right shows a small fragment after magnification by  $\delta_1$  and  $\delta_2$  along the horizontal and the vertical axes, respectively. The following color codes are used. For the left picture: 2 - green, 4 - yellow, 8 - violet, 16- red, 6 - pink, 12 - light blue; for the right picture the same colors correspond to the quadrupled periods: 8 - green, 16 - yellow, 32 - violet, 64- red, 24 - pink, 48 - light blue.

Fig. 17. The universal two-dimensional pattern of the parameter plane topography near a critical point with the period-3 code  $UUDUUD\dots$ . The critical point is located in the center of the pictures. The left picture shows the interior of the parallelogram labeled "3" in Fig. 14. Scaling coordinates  $(C_1, C_2)$  are used here (see Eq.(15)). The right picture shows a small fragment after magnification by  $\delta_1$  and  $\delta_2$  along the horizontal and the vertical axes, respectively. The following color codes are used. For the left picture: 2 - green, 4 - yellow, 8 - violet, 16- red, 6 - pink, 12 - light blue; for the right picture the same colors correspond to the periods multiplied by 8: 16 - green, 32 - yellow, 64 - blue, 128- red, 48 - pink, 96 - light blue.

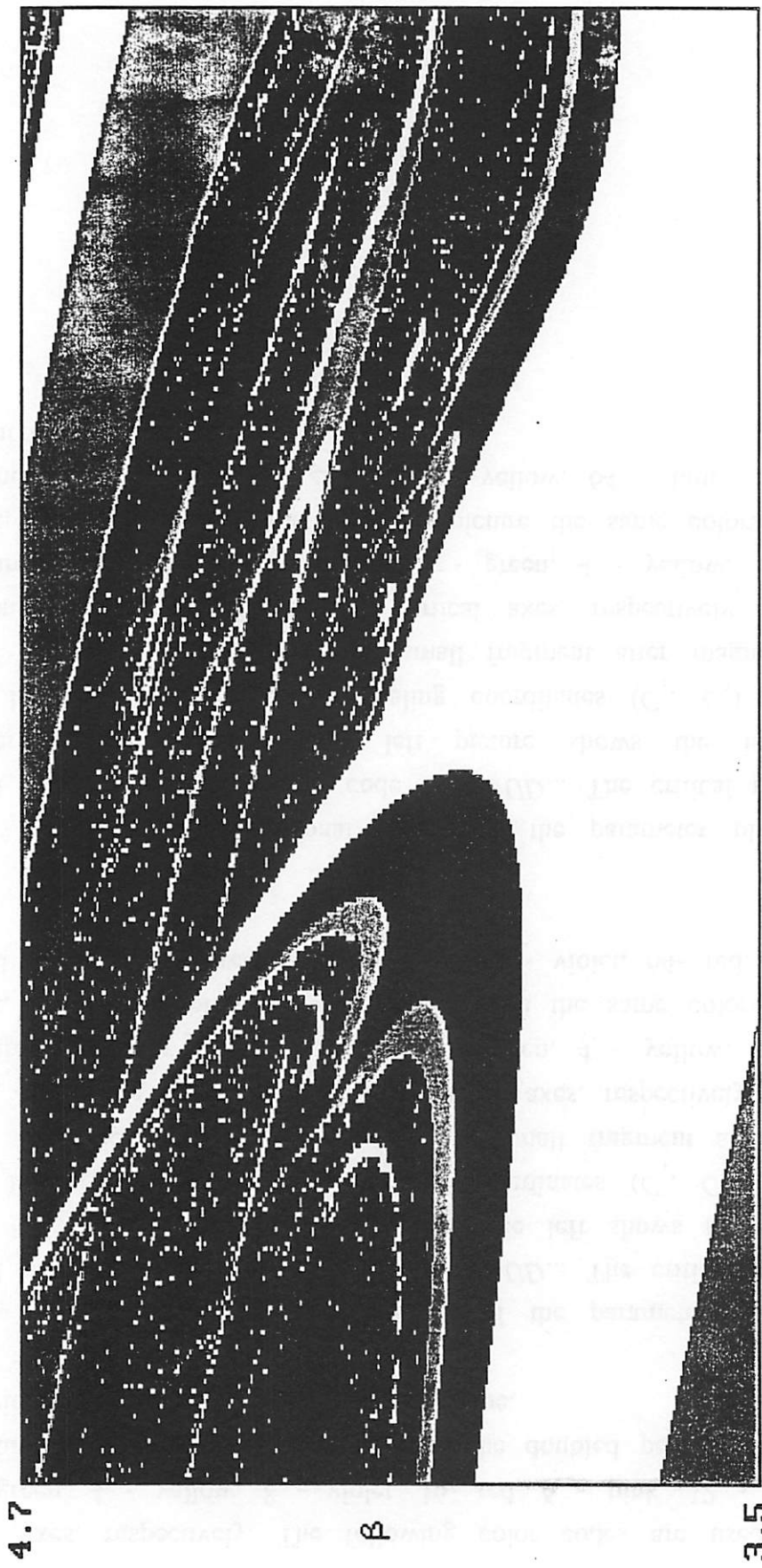


Figure 1(a)

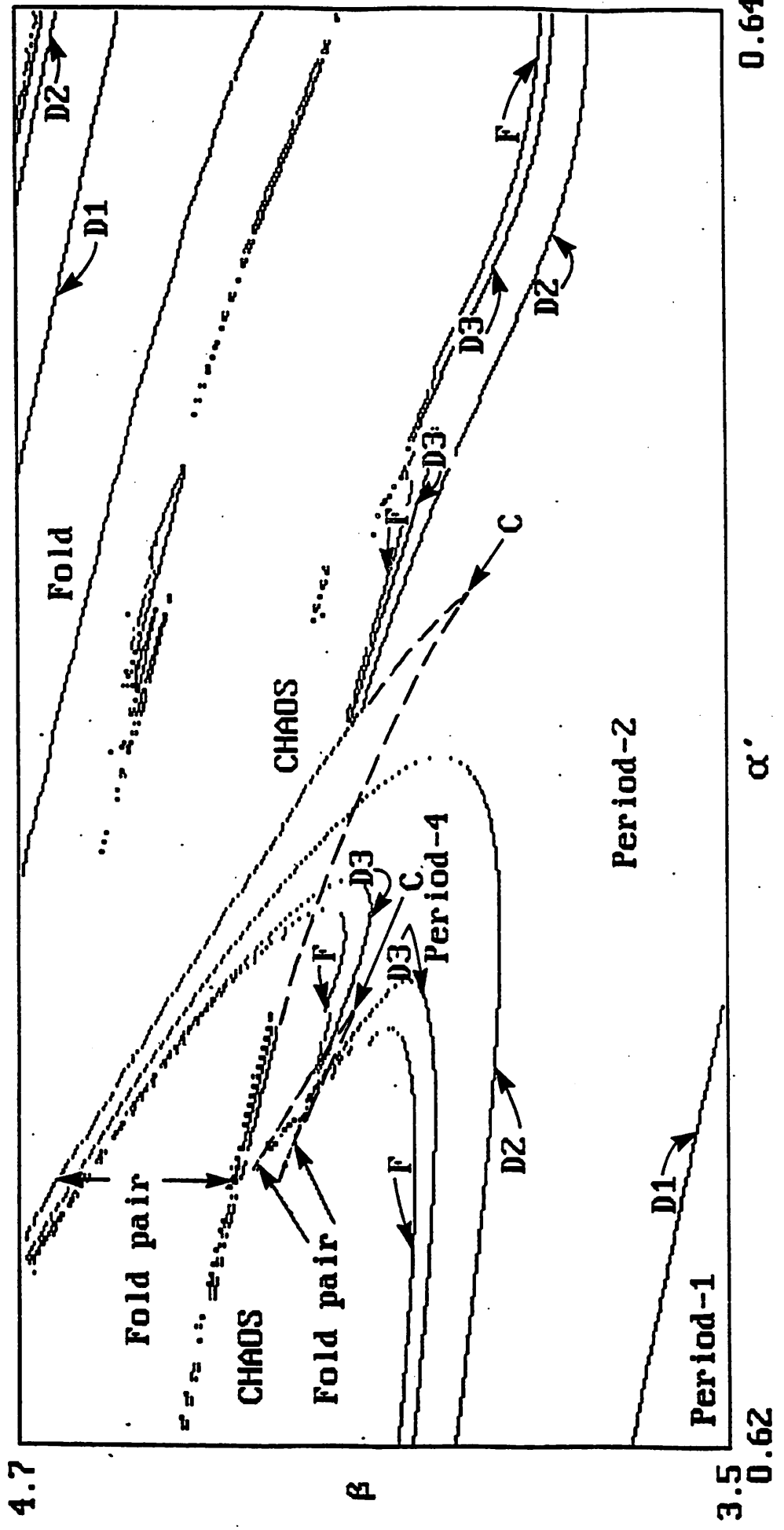


Figure 1(b)

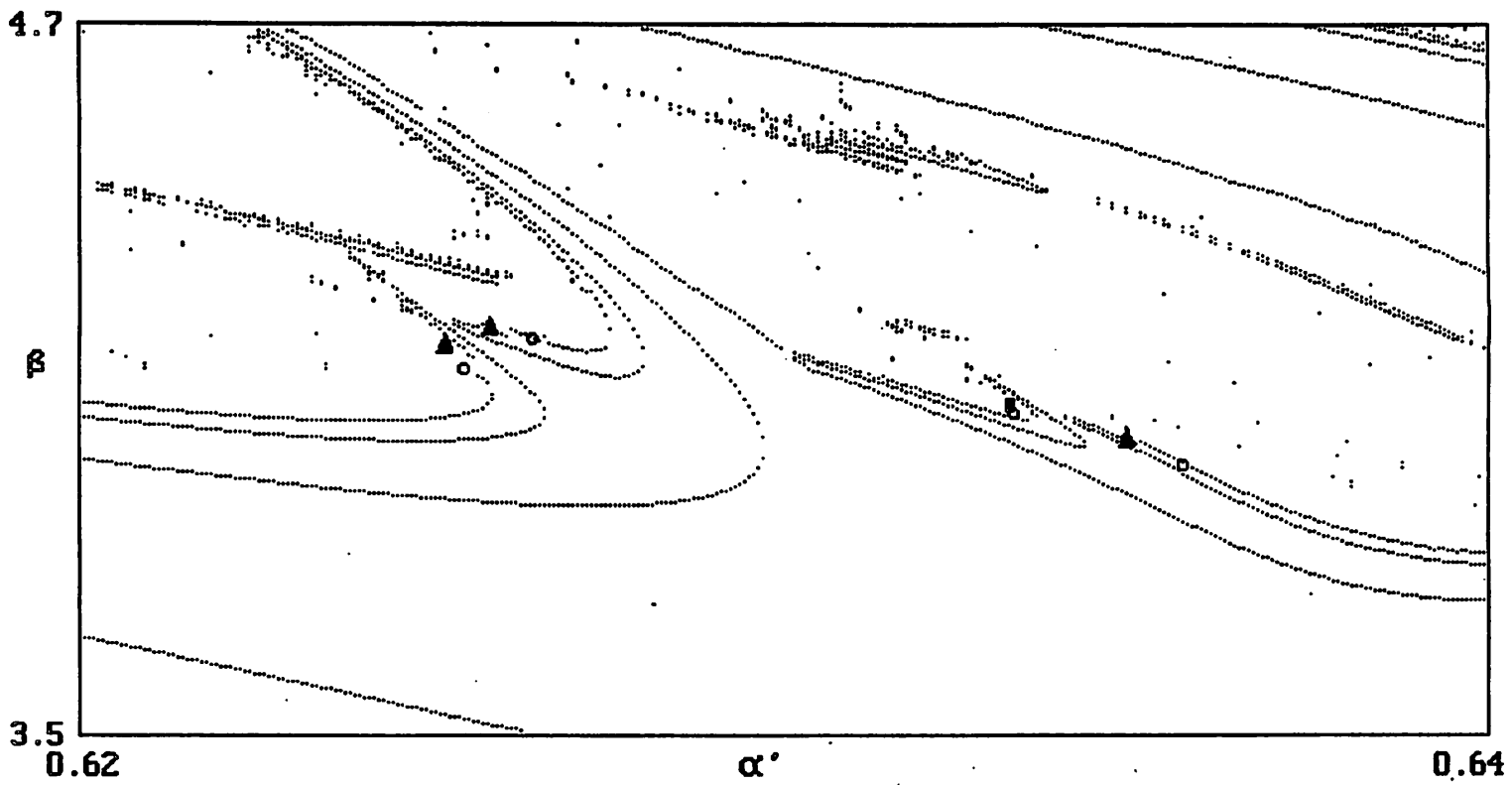


Figure 1(c)

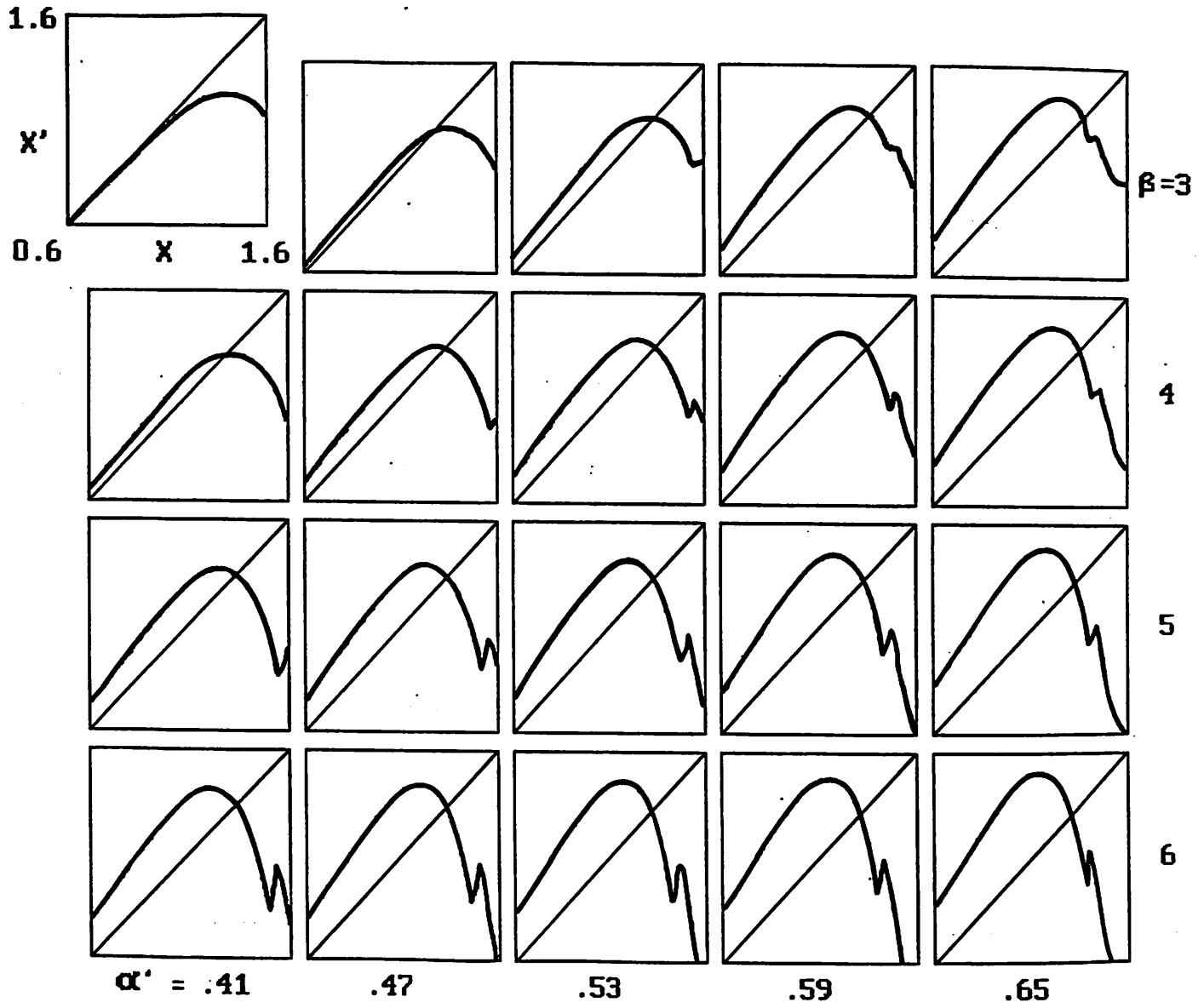


Figure 2

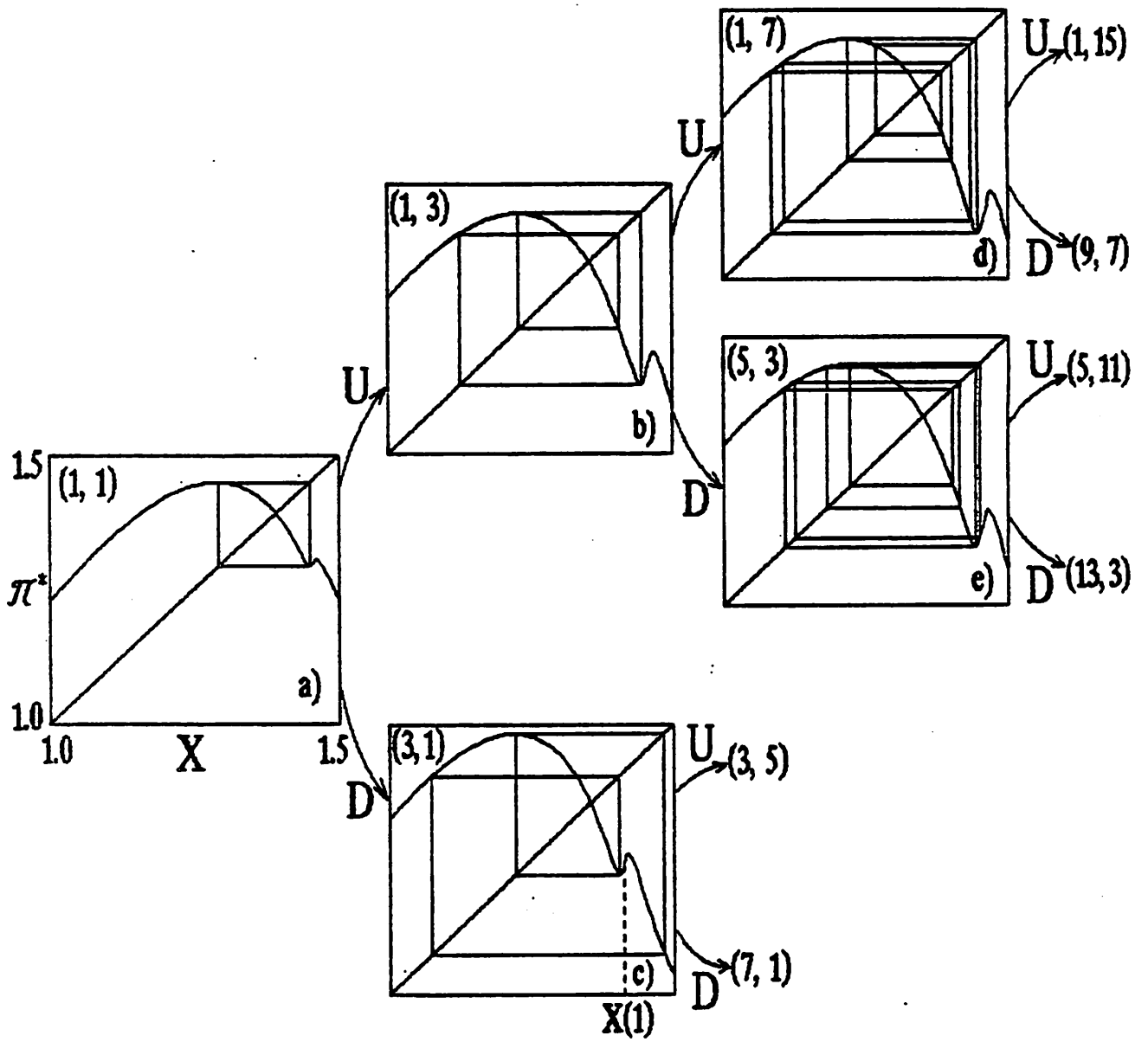


Figure 3

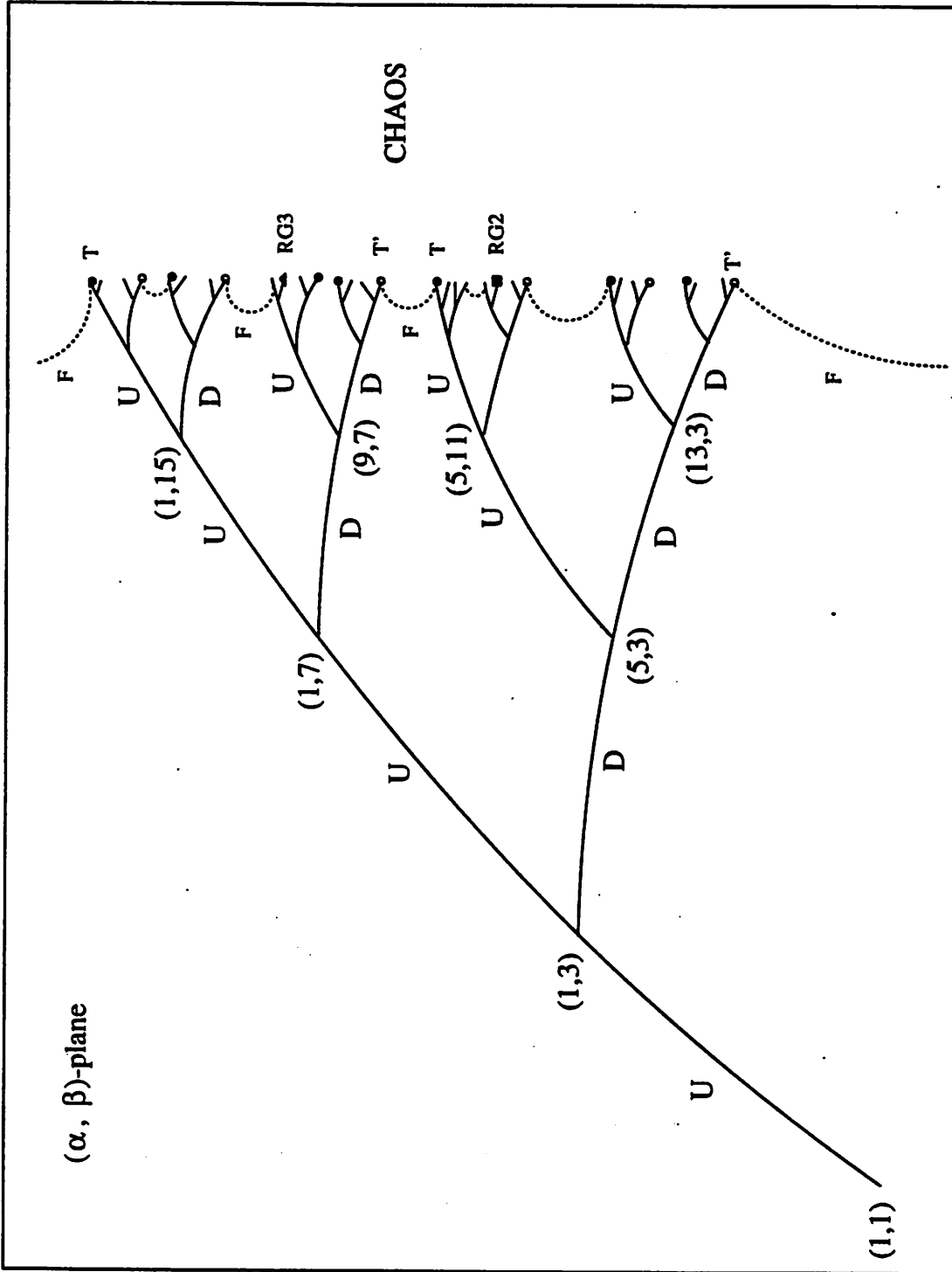


Figure 4

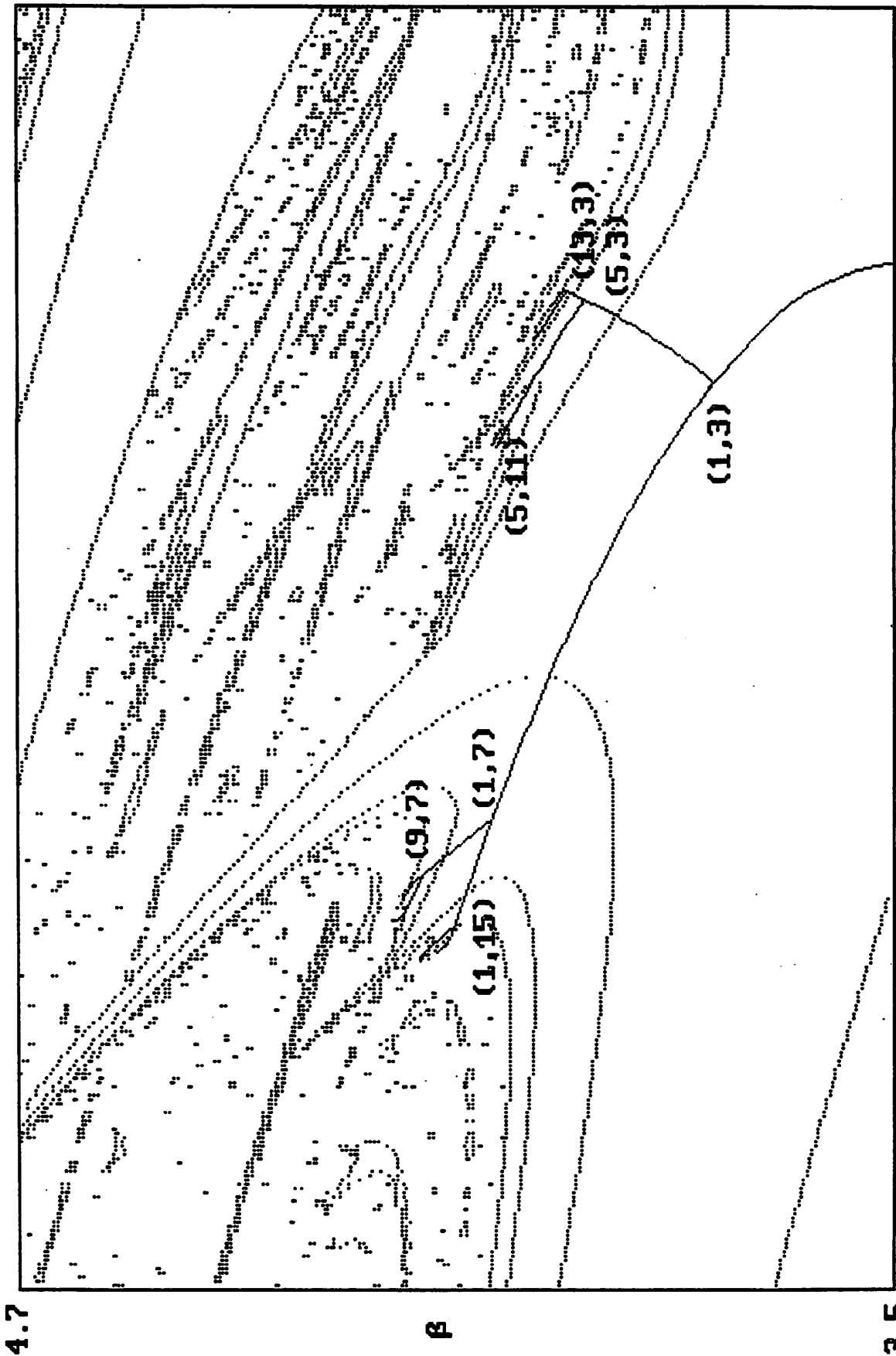


Figure 5

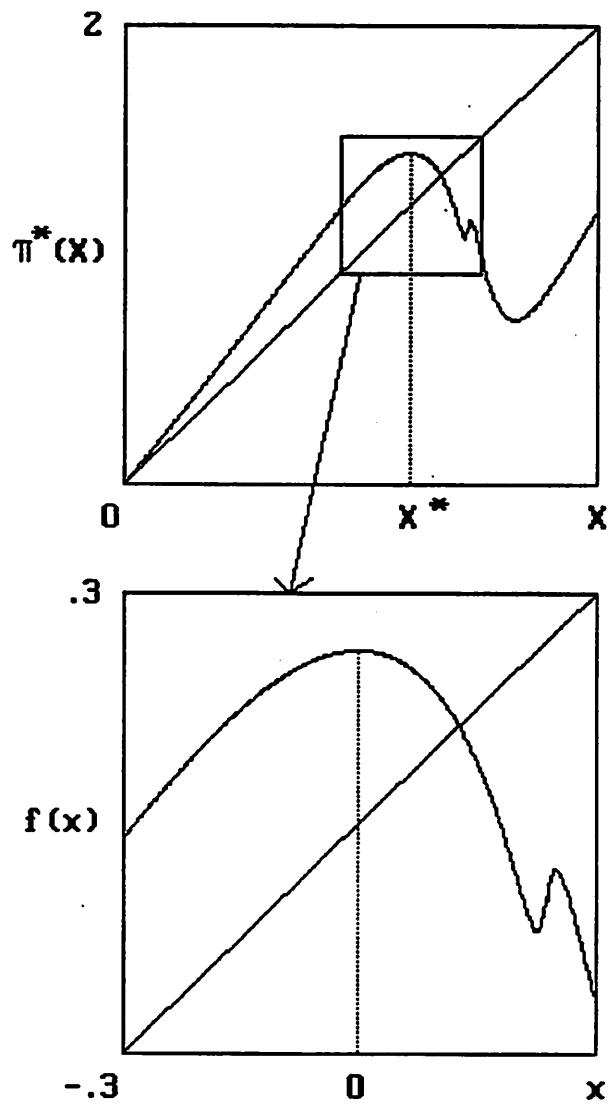


Figure 6(a), (b)

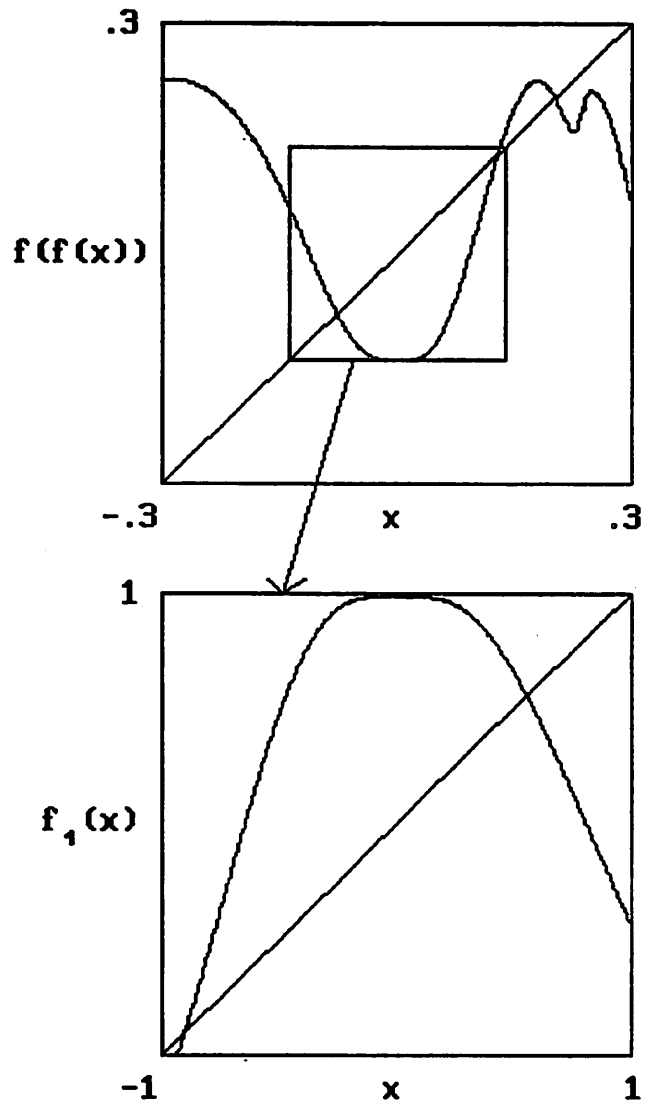


Figure 6(c), (d)

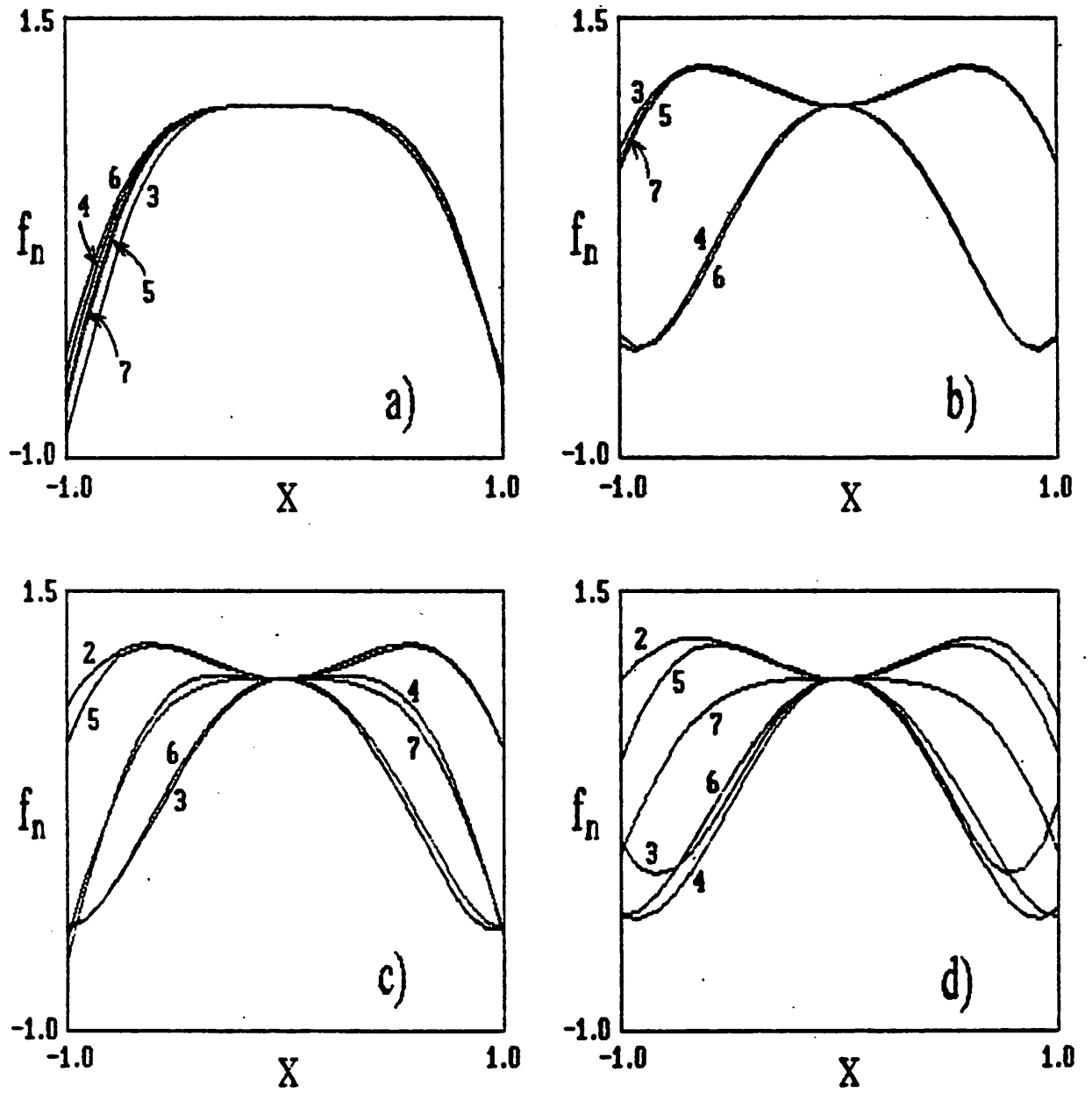
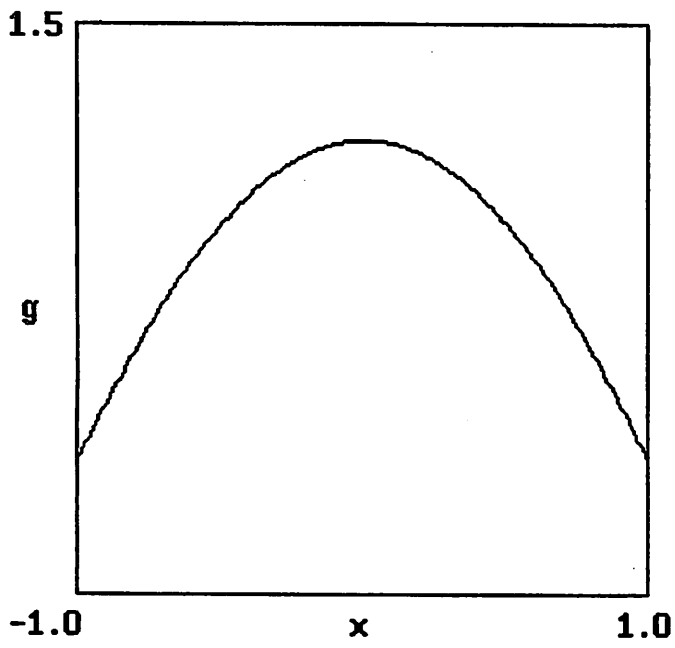
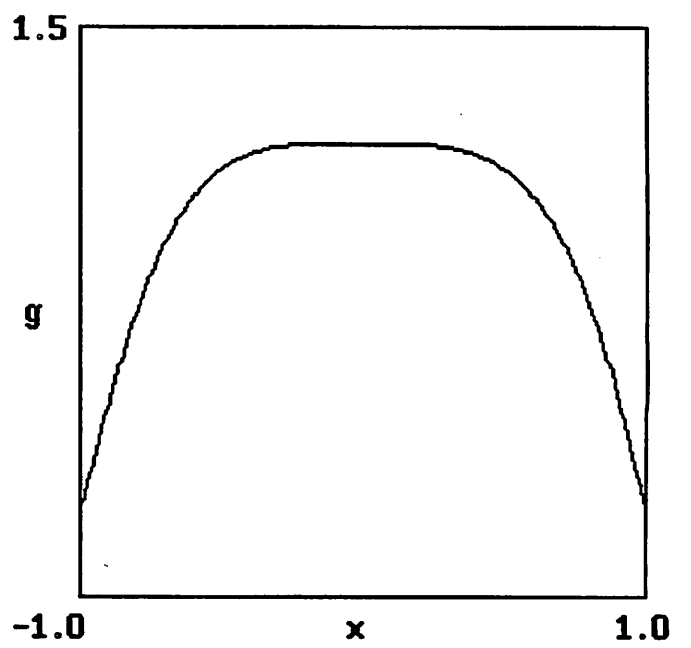


Figure 7

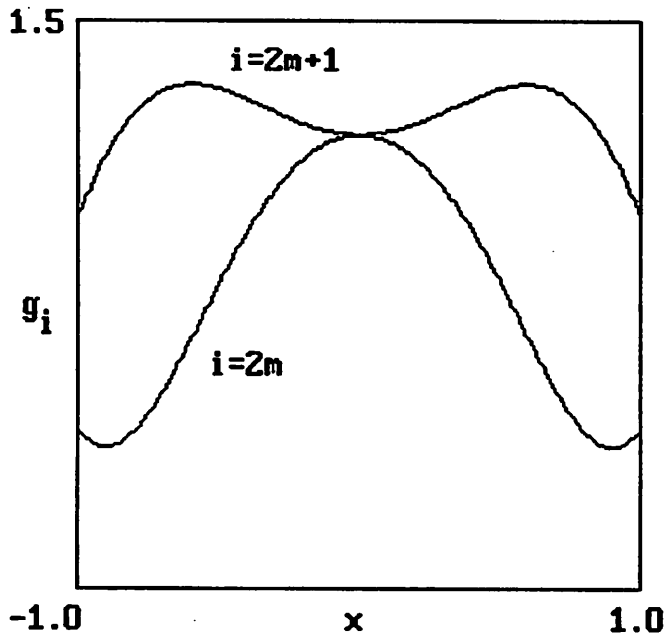


(a)

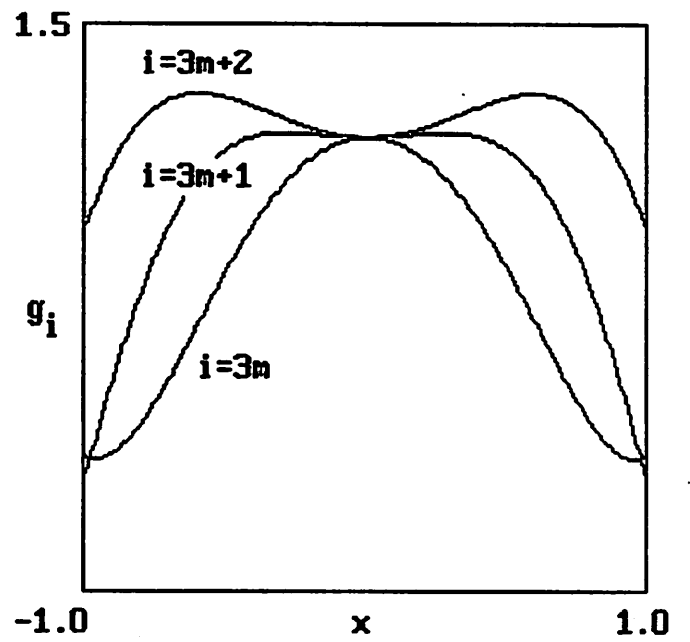


(b)

Figure 8(a), (b)



(c)



(d)

Figure 8(c), (d)

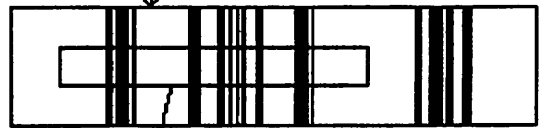
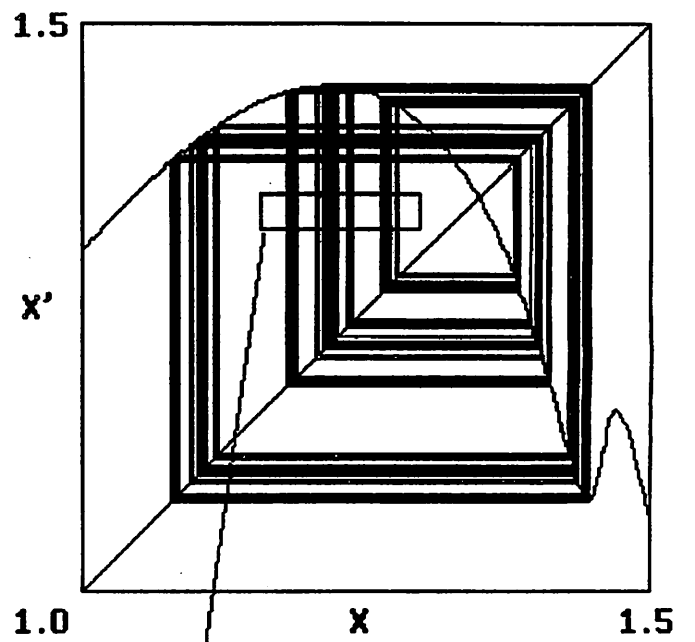
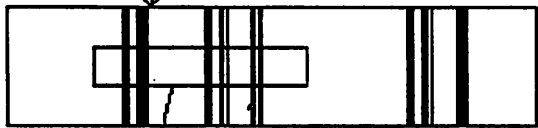
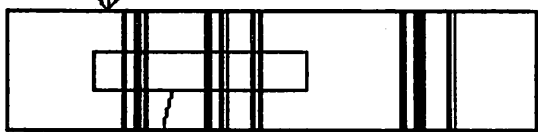
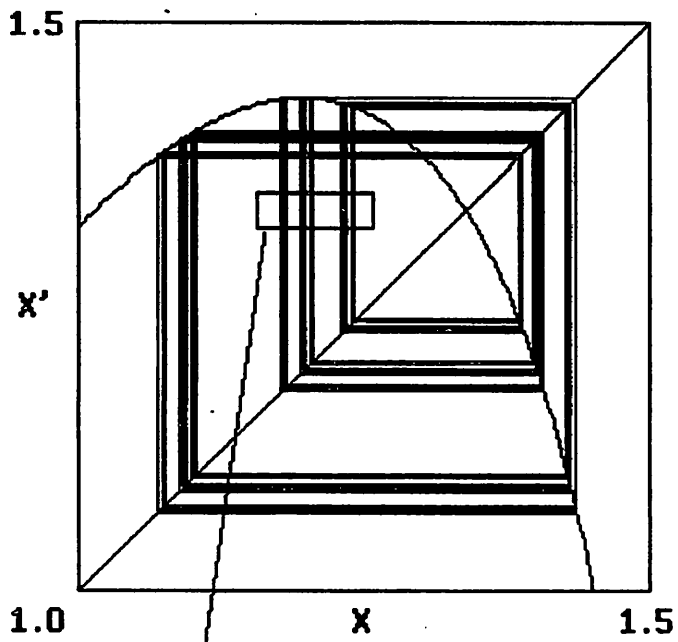


Figure 9(a), (b)

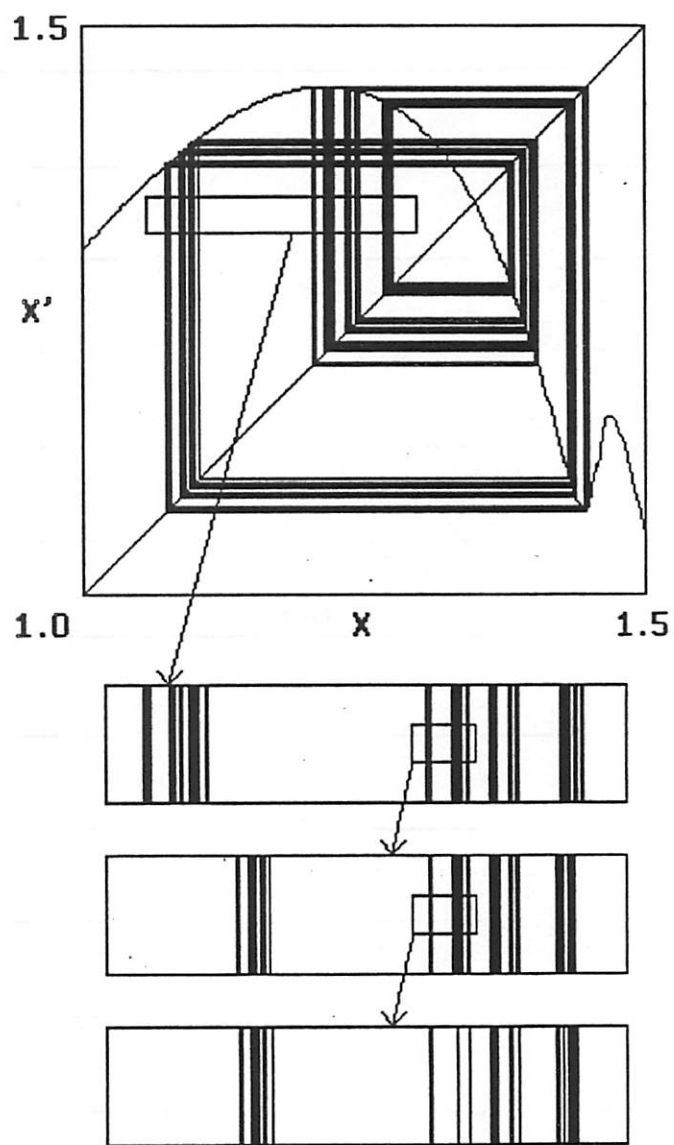
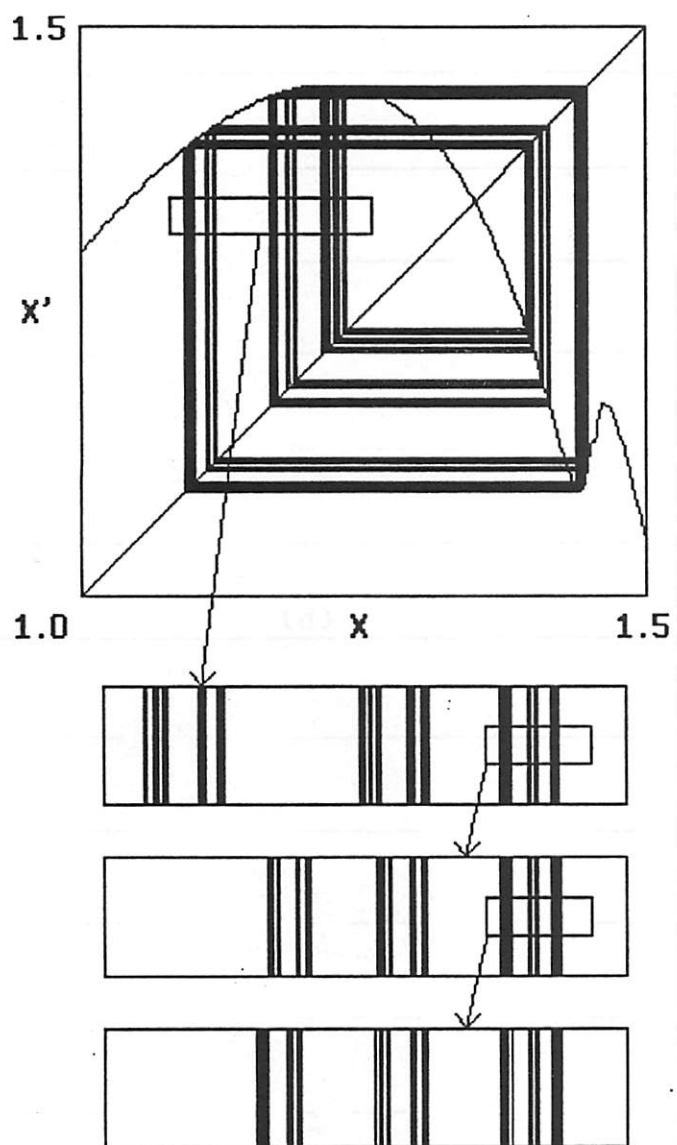


Figure 9(c), (d)

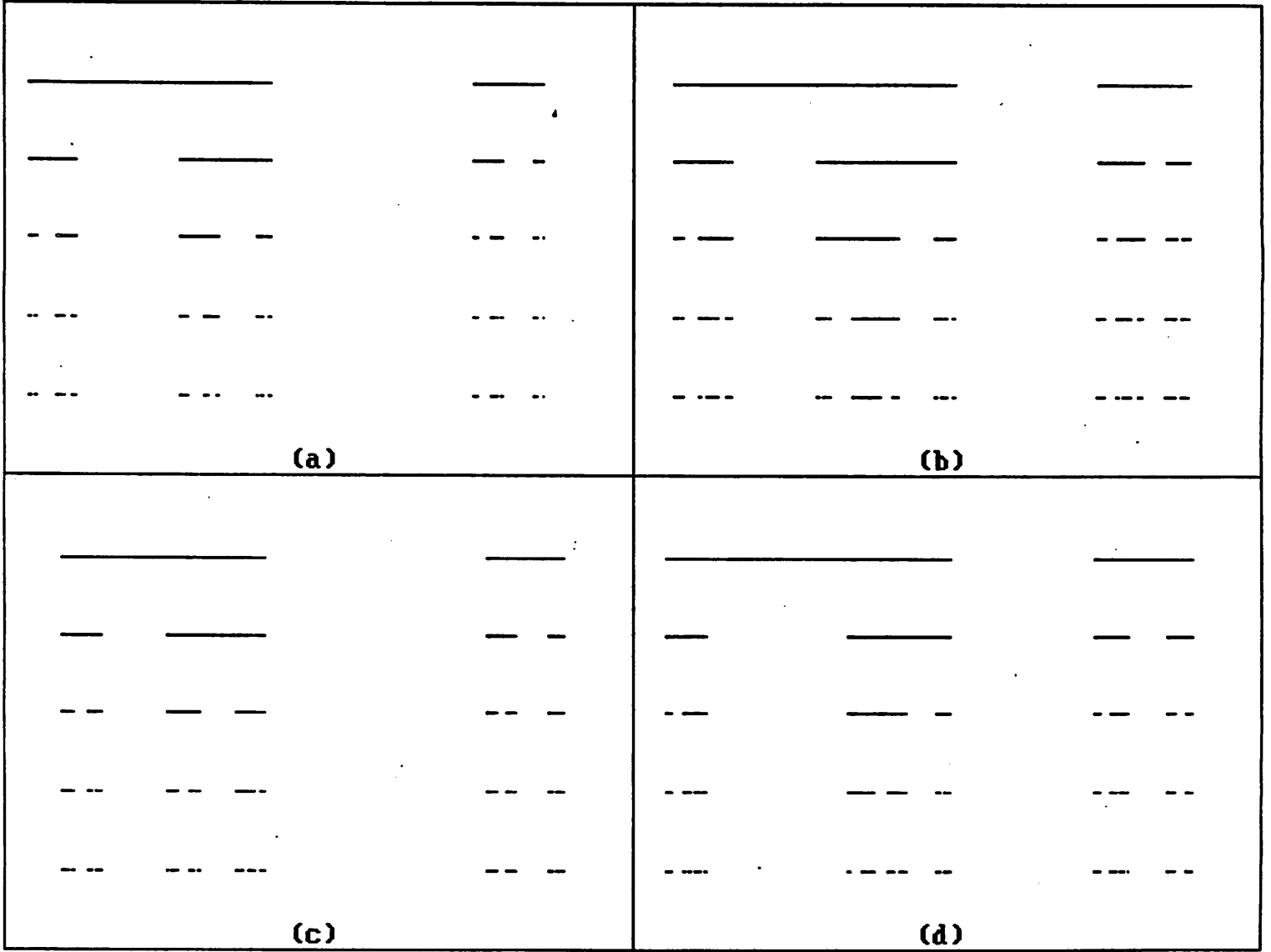


Figure 10

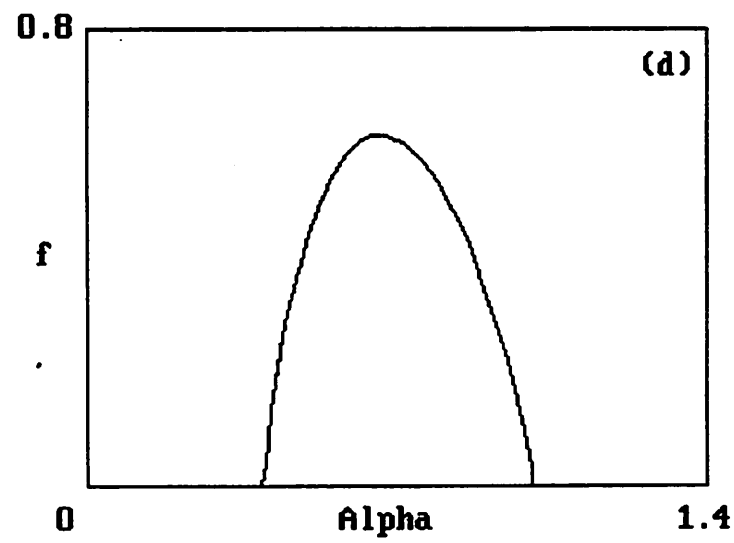
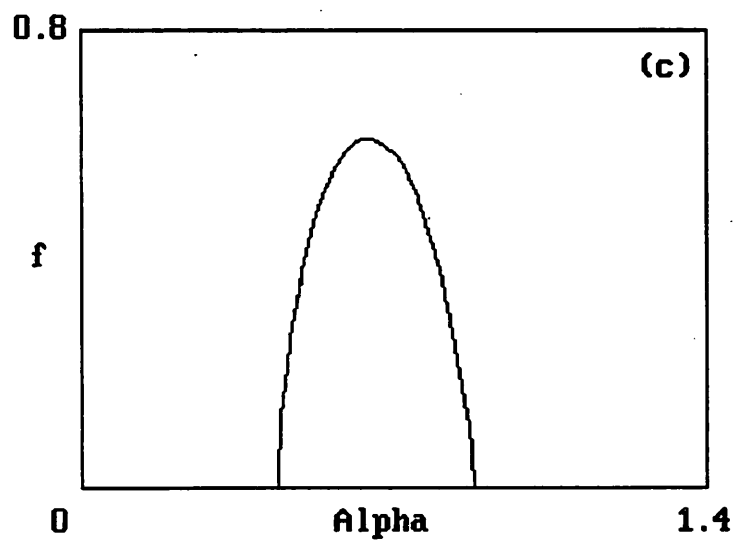
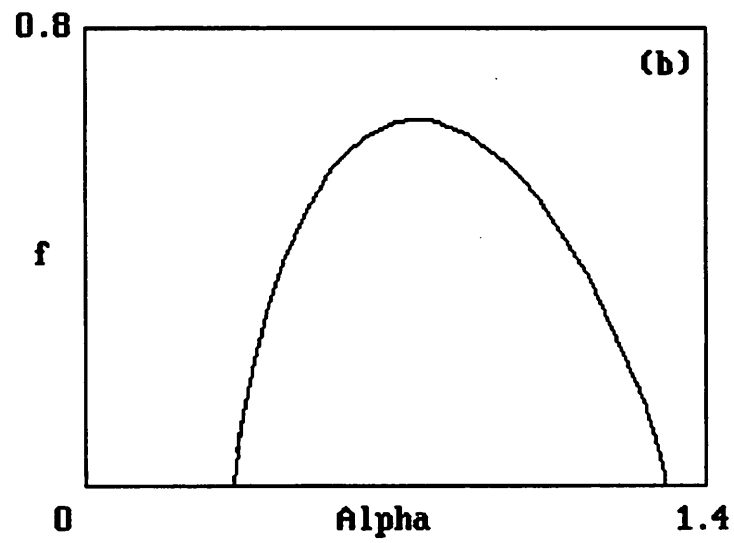
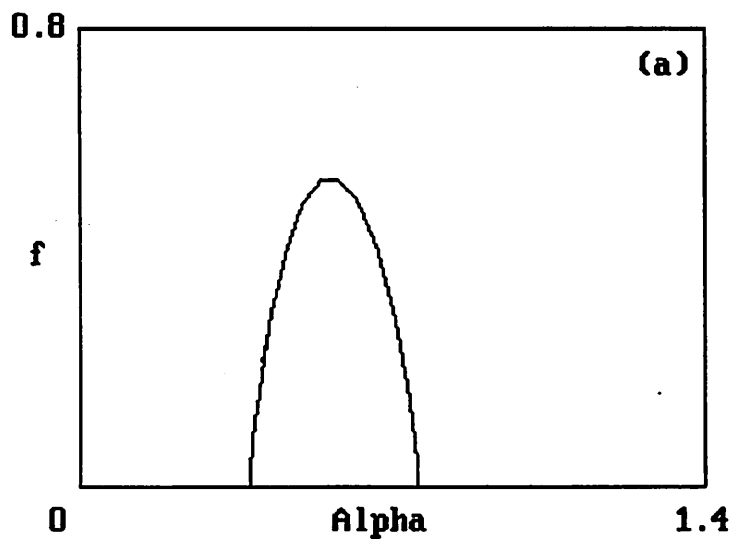


Figure 11

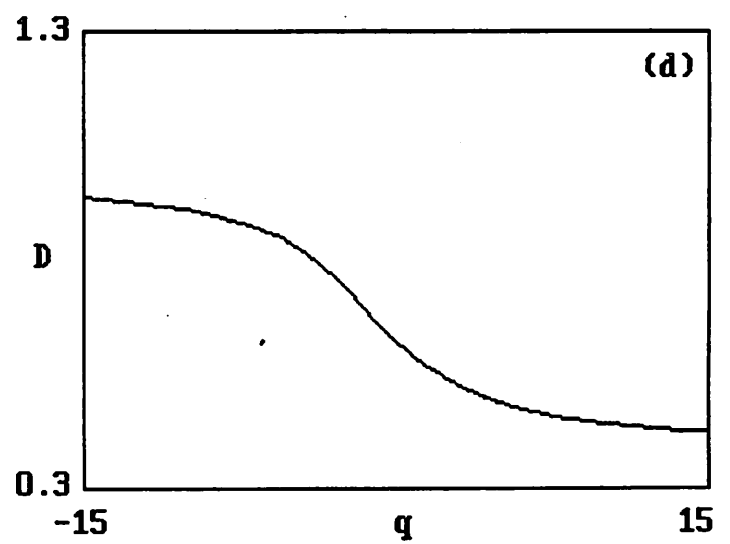
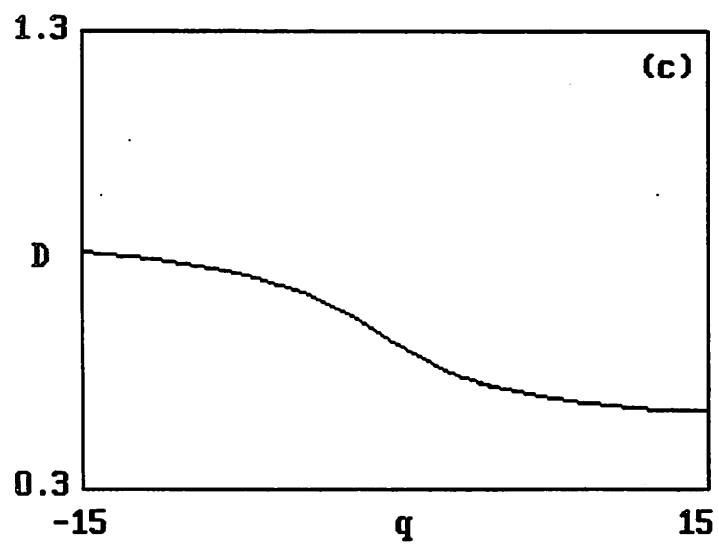
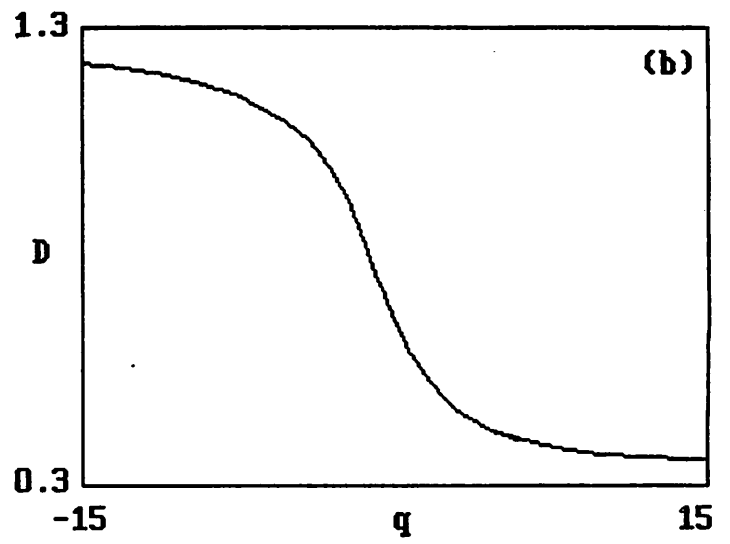
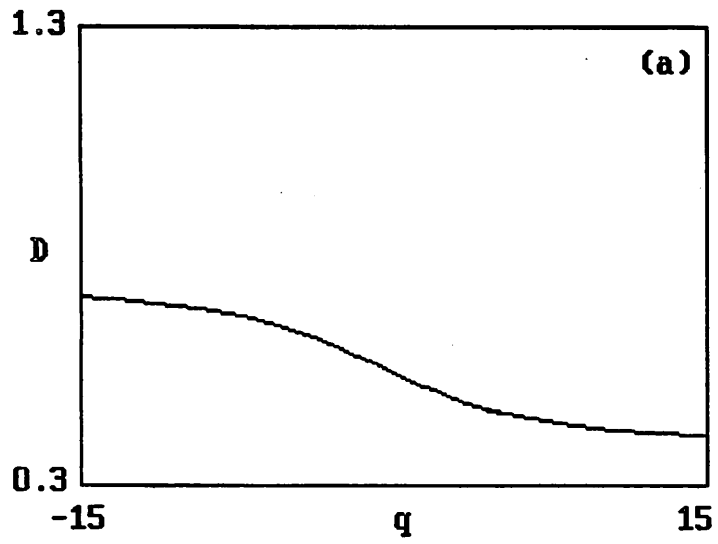
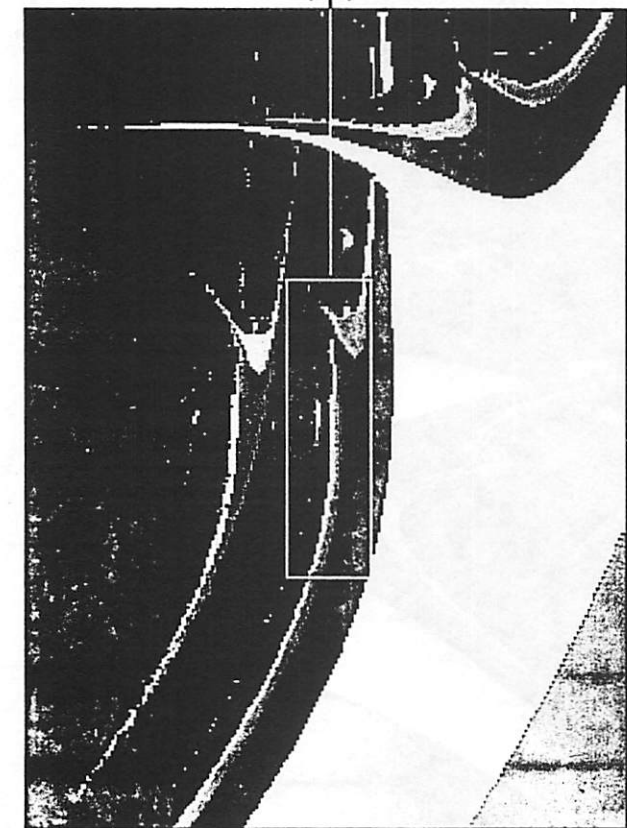
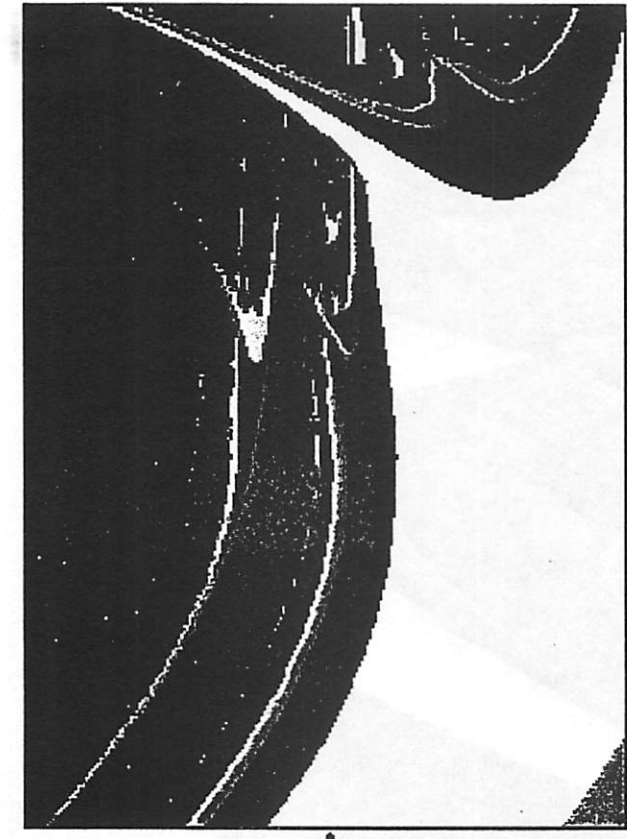


Figure 12



.15

$C_1$

-.15

$C_2$

.15

Figure 15

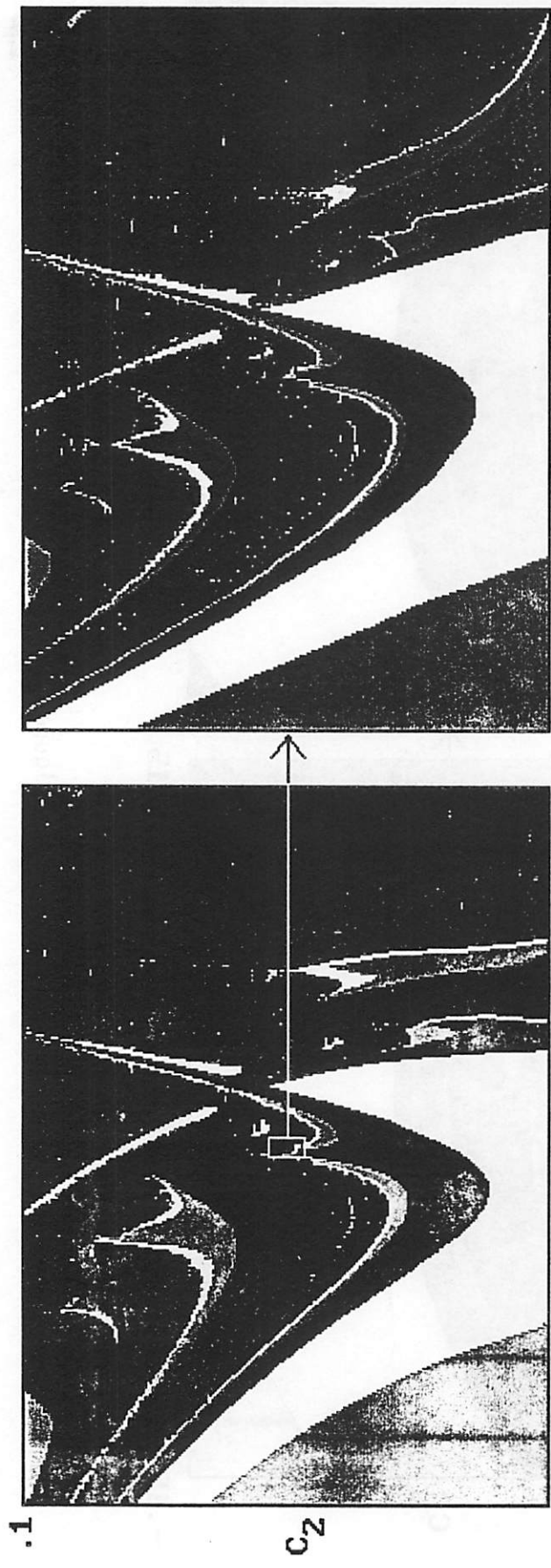


Figure 16

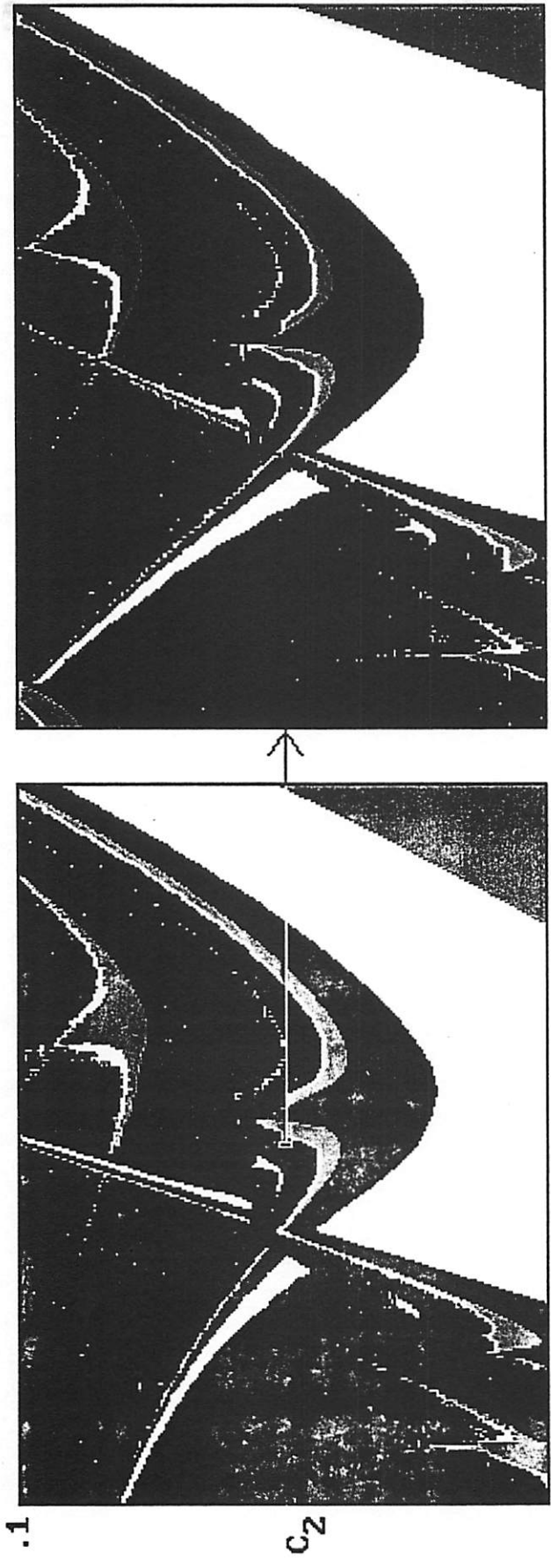


Figure 17